Nonlinear optical properties of pyrimidine chromophores

Michaela Fecková,[a,b] Pascal le Poul,[a] Filip Bureš,[b] Françoise Robin-le Guen,[a] Sylvain Achelle.[a,*]

[a]Univ Rennes, CNRS, ISCR (Institut des Sciences Chimiques de Rennes) - UMR 6226, F 35000 Rennes, France. E mail: sylvain.achelle@univ-rennes1.fr

[b]Institute of Organic Chemistry and Technology, Faculty of Chemical Technology, University of Pardubice, Studenská 573, Pardubice 53210, Czech Republic.

Abstract

The large library of nonlinear optical (NLO) chromophores based on pyrimidine scaffold is discussed in this review. Since the first examples described thirteen years ago, the interest in pyrimidine push-pull NLO chromophores has increased dramatically, especially for second harmonic generation and two photon absorption. More than 130 properly selected chromophores are presented to demonstrate fundamental structure-property relationships and to highlight key applications of pyrimidine-derived materials.

Keywords: Pyrimidine; Two-photon absorption; Second harmonic generation; Nonlinear optic

Introduction

Nonlinear optics (NLO) was initially studied theoretically by Maria Göppert-Mayer when she was a PhD student at the University of Göttingen.[1] Experimentally, the NLO began to be studied in the 1960s shortly after the development of lasers: a sufficiently powerful source of coherent light. In 1961, Franken *et al.* reported for the first time the phenomenon of second harmonic generation (SGH) with a quartz crystal irradiated at λ_0 = 694,3 nm with ruby laser leading to emission of the UV light with doubled frequency (λ_2 = 347,2 nm).[2] In the same

Accepted manuscript

year, two-photon absorption (TPA), a third-order NLO process, was discovered by Kaiser and Garret.[3] Third harmonic generation (THG), another third order NLO phenomena, was observed at λ_3 = 231,4 nm with the same ruby laser previously used for SHG, later by Terhune *et al*.[4]

On a microscopic scale, when an electromagnetic field $\vec{E}$ interacts with a molecule, a polarization resulting in induced dipolar moment $\vec{\mu}$ is given by the following equation:

$$\vec{\mu} = \overrightarrow{\mu_0} + \alpha\overrightarrow{E^1} + \beta\overrightarrow{E^2} + \gamma\overrightarrow{E^3} + \cdots \quad \text{Eq. 1}$$

Where :

- $\overrightarrow{\mu_0}$: the electrical dipolar moment of the molecule in ground state
- α : the linear polarizability tensor
- β : the second order (quadratic) hyperpolarizability tensor
- γ : the third order (cubic) hyperpolarizability tensor

On a macroscopic scale, the polarization $\vec{P}$ of the material can be written:

$$\vec{P} = \overrightarrow{P_0} + \sum_i \chi^{(i)}\overrightarrow{E^i} = \overrightarrow{P_0} + \chi^{(1)}\overrightarrow{E^1} + \chi^{(2)}\overrightarrow{E^2} + \chi^{(3)}\overrightarrow{E^3} + \cdots + \chi^{(n)}\overrightarrow{E^n} \quad \text{Eq.2}$$

Where :

- $\overrightarrow{P_0}$: intrinsic polarization of the material
- $\chi^{(1)}$: linear (1st order) susceptibility tensor
- $\chi^{(2)}$, $\chi^{(3)}$ and $\chi^{(n)}$: 2nd order (quadratic), 3rd order (cubic), and *n*th order non linear susceptibility tensors.

The β and γterms are related to 2nd and 3rd order NLO respectively. NLO effects are only observed for high intensity electric field $\vec{E}$, otherwise *n* order term are not significant and the polarization can be considered as linearly dependent on $\vec{E}$. It should be noted that $\chi^{(2)}$ and β terms are null in case of centrosymmetric materials or molecules.[5] On the other hand, $\chi^{(3)}$ and γ terms are always present even if not always observable.

Accepted manuscript

Even if numerous inorganic NLO materials such as lithium niobate have been initially used, organic and organometallic derivatives emerged during the past four decades, mainly due to their higher and faster NLO response as well as better tunability.[6]

Concerning the 2nd order NLO, the main applications are based on the sum frequency generation,[7] mainly SHG, Pockels effect and optical rectification.[8] The most investigated application involves conversion of red laser into a blue/green coherent source of light used for example in the Blu-Ray© technology.[9] Other key applications are related to optical signal processing and integrated optics[10] as well as SHG microscopy.[11] The β tensor is generally expressed in esu (1 esu ≈ 3.34 10^{-11} C). Three main methods are used to measure the molecular 2nd order NLO response. The first one is the electric field induced second harmonic generation (EFISH), the second one is the hyper Rayleigh scattering (HRS),[12] while harmonic light scattering (HLS) can also be used.[13] The HRS and HLS methods provide directly the β tensor in the three directions of space with Cartesian coordinates. This method permits to measure NLO response even if the molecule does not present any permanent dipolar moment such as octupolar compounds. The EFISH method can be applied to non-charged polar molecules and is based on the application of a high external electric field $\vec{E}$ on the analytical cell to align the chromophores in the same direction. This method provides the NLO response as the scalar product between the permanent dipolar moment of the molecule $\vec{\mu}$ in fundamental state and the vector component of β described as $\beta_{//}$. Dispersion of β, in particular for linear push-pull molecules, can be described by a two-state model according to the following equation:[14]

$$\beta_0 = \beta\left(1-\left(\frac{\lambda_{max}}{\lambda}\right)^2\right)\left(1-\left(\frac{2\lambda_{max}}{\lambda}\right)^2\right) \quad \text{Eq. 3}$$

The D-π-A push-pull arrangement is typical of 2nd order NLO chromophores and the value of the β tensor is closely related to the intramolecular charge transfer (ICT) into the molecule,

Accepted manuscript

which can be tuned by varying the donor (D)/acceptor (A) pair interconnected by a π-conjugated linker. On a macroscopic scale, 2nd order NLO/electro-optic materials formed by chromophores dissolved in a polymer matrix, can be obtained by electro-poling. The chromophores are oriented via an external electric field at the temperature elevated above the glass transition temperature of the used polymer matrix and cooled with persistent electric field.[15]

As far as the 3rd order NLO response is concerned, the imaginary part of the γ term is related to multiphoton absorption including TPA: two photons can be absorbed simultaneously by a molecule.[16] The real part of γ will induce the Kerr effect leading to change in the refractive index as a response to the applied electric field. The main applications of TPA span biological imaging,[17] microfabrication,[18] optical limiting,[19] 3D optical data storage[20] and TPA photodynamic therapy.[21] On the other hand, the Kerr effect is used for all optical data processing.[22] TPA cross-section, expressed in Göppert-Mayer unit (GM = 10^{-50} cm^4.s.photons^{-1}) can be measured by the Z-Scan or the two-photon excitation fluorescence (TPEF) methods. The TPEF technique is based on upconverted fluorescence emission.[23] The Z-scan technique is suitable for non-fluorescent materials as it relies on transformation of phase distortion to amplitude distortion during beam propagation through a nonlinear medium.[24] Both open- and closed-aperture Z-scan methods can be used for TPA characterization. Closed-aperture Z-scan can also be employed for measuring the real part of the γ tensor.[25] In case of D-π-A push pull derivatives, the TPA maximum is observed exactly at the double of one-photon absorption maxima, but in case of quadrupolar or octupolar structures, the TPA maxima are generally observed at a lower wavelength than the double of one-photon absorption maxima. In these cases, the lowest energy excitation is theoretically two-photon forbidden.[26] In general, the branching effect, with quadrupolar and octupolar structures, significantly enhances the TPA cross-section.[27] TPA properties are highly solvent

Accepted manuscript

dependent: the values of TPA cross section plotted versus the solvent polarity generally show a non-monotonic dependence and can be hardly modeled. On the other hand, theoretical calculations can be very useful to predict and rationalized the NLO properties of organic chromophores.

The pyrimidine ring, also called 1,3-diazine, is a six membered heterocycle with two nitrogen atoms in positions 1 and 3. This heterocycle is present within the structure of many natural and biologically active products[28] and pyrimidine scaffold can also be found in cytosine, thymine and uracil nucleobases. Pyrimidine is a π-deficient heterocycle and the pyrimidin-4-yl and the pyrimidin-2-yl fragments are therefore electron-withdrawing groups as shown by their Hammett constants (σ_P = 0.63 and 0.53), close to the cyano group (σ_P = 0.66).[29] Due to the position of the nitrogen atoms, these fragments exhibit a stronger electron accepting character than other diazinyl moieties. Many push-pull pyrimidine derivatives exhibit interesting optical properties.[30] The electron-withdrawing character of the pyrimidinyl fragment induces a strong emission solvatochromism observed for π-conjugated pyrimidine derivatives substituted by electron-donating groups.[31] Engaging the electron lone pairs of the nitrogen atoms of pyrimidine by protonation,[32] complexation,[33] or *N*-methylation[34] is an easy and useful way to further increase the electron-withdrawing character of the pyrimidine core. The synthesis of π-conjugated pyrimidine chromophores is now well established and is often based on functionalization of commercially available pyrimidine building blocks by palladium catalyzed cross coupling reactions[35] or condensation reactions.[36] Many halogen-substituted and methyl substituted pyrimidines are indeed readily available. Moreover, pyrimidine functionalization is often more tunable and selective than in case of well-known 1,3,5-triazine core.[37]

In this contribution, we will summarize various examples of pyrimidine NLOphores described during the last fifteen years and try to highlight the key structural parameters that

Accepted manuscript

affect their NLO properties. The main applications of pyrimidine NLOphores will also be briefly highlighted. The first part of the review will focus on 2nd order NLO properties, while the 3rd order, mainly TPA, properties will be discussed subsequently.

2nd order NLO properties

This chapter focuses on pyrimidines with second order NLO properties that are generally measured in solution using EFISH, HRS or HLS techniques. The discussed derivatives are sorted into groups according to their structural similarities. The main aim of this chapter is to discuss and confront the following structural features: i) electron-donating group, ii) length and arrangement of the π-conjugated linker, iii) *N*-complexation or quaternization of the heterocycle, iv) the number of arms attached to the pyrimidine central core.

4-Styrylpyrimidines **1** (Figure 1) were synthetized in our lab as model push-pull molecules capable of further *N*-complexation with tungsten carbonyl or *N*-methylation leading to **2** and **3**. Their fundamental nonlinear optical properties such as $\mu\beta$ and $\mu\beta_0$ are summarized in Table 1. Chromophores in series **1**, compounds **1a**, **1b** and **1e** in particular, vary in the electron donor, which significantly affects the measured $\mu\beta$ and $\mu\beta_0$ products. These values follow the electron releasing strength of the particular donors within the order of diphenylamino < piperidine < dimethylamino and are consistent with the theoretical calculations.[38] The diphenylamino group in **1b** and **1d** decreases the $\mu\beta$ values even though this group lowers the ICT energy, which is most likely due to a partial delocalization of the amino lone electron pair into two appended phenyls, while the lower donor strength shifts the ground-state to a less favorable bond alternation.[38a] However, the calculated bond length alternation (BLA) values of the vinylic linker are similar and, therefore this phenomenon would needs further investigation. [38c] A coordination of the pyrimidine ring by tungsten pentacarbonyl afforded **2a**-**d** with significantly improved NLO responses (Table 1). Moreover, *N*-methylation as in

Accepted manuscript

3b, **3d** resulted in increased $\mu\beta$ by a factor of 5–12.[38b] Both modifications alter the pyrimidine electron-withdrawing character, $W(CO)_5$ caused formation of a new low-lying metal to ligand charge-transfer (MLCT) transition, which is mostly responsible for increased NLO response.[38b] Stronger donors caused better NLO response, however the trend in π-linker extension is rather opposite to that observed for parent **1**.

Table 1: 2nd order NLO response of chromophores **1–3** measured by EFISH method

Compds	λ_{abs} (nm)[a]	$\mu\beta$,[b] 10^{-48} esu	$\mu\beta_0$,[c] 10^{-30} esu	Ref
1a	393	330	262	38a
1b	400	190	150	38a
1c	386	470	377	38a
1d	384	200	161	38b
1e	386	290	233	38a
2a	462	770	555	38b
2b	462	700	504	38b
2c	443	490	363	38b
2d	435	460	345	38b
3b	564	2350	1394	38b
3d	520	1080	702	38b

[a] Measured in CH_2Cl_2, [b]Measured in $CHCl_3$ at 1907 nm [c]Two level corrected β value.[14]

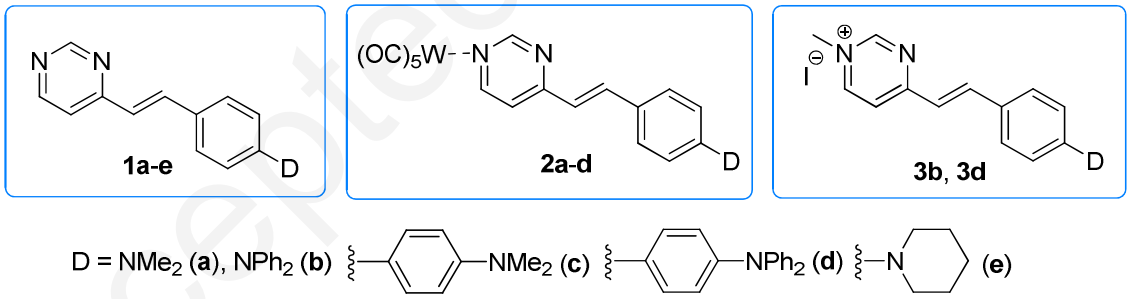


Figure 1 Structures of 4-styrylpyrimidines **1–3**

Influence of mesomeric donors such as NMe_2, NPh_2 and MeO along with the π-system composition on NLO activity has been screened in 4-styrylpyrimidines **4** and **5** (Figure 2, Table 2).[39] Well-evaluated series **5a-c** showed a clear trend in increased $\mu\beta$ when going from OMe to NPh_2 and NMe_2 donors. It is well-known that 2,5-thienylene unit allows efficient intramolecular charge-transfer (ICT) due to its lower resonance energy as compared to

Accepted manuscript

1,4-phenylene one.[40] However, its influence in chromophores **4** and **5** is less straightforward and depends on the used donor. Whereas weaker NLO response has been recorded for *N*,*N*-dimethylamino-substituted chromophore **5a** (compared to **4a**), in the *N*,*N*-diphenylamino series **b** is the situation opposite.

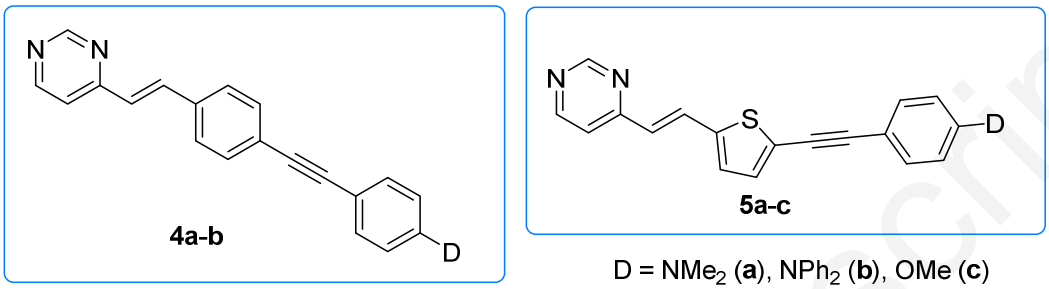


Figure 2 2,5-Thienylene vs. 1,4-phenylene linkers in styrylpyrimidines

Table 2: 2nd order NLO response of chromophores **4–5** measured by EFISH method

Compds	λ_{abs} (nm)[a]	$\mu\beta$,[b] 10^{-48} esu	$\mu\beta_0$,[c] 10^{-30} esu	Ref
4a	491	560	446	39
4b	494	280	222	39
5a	419	440	338	39
5b	416	400	308	39
5c	484	150	121	39

[a] Measured in CH_2Cl_2, [b]Measured in $CHCl_3$ at 1907 nm [c]Two level corrected β value.[14]

NLOphores with push-pull arrangement based on an aromatic scaffold have been extensively studied.[41] However, the aromatic arrangement is preferred in the ground state and the ICT in aromatic D-π-A systems generally causes loss of the resonance energy. This contradiction reduces effective donor-acceptor coupling and potential NLO response.[42] Employment of a pro-aromatic unit/donor, which is capable to gain aromaticity upon the ICT, seems to be very smart solution to overcome this issue. Hence, we have prepared a series of pyrimidine/pyrimidinium chromophores **6/7** (Figure 3, Table 3) bearing pyranylidene proaromatic fragment, and investigated their NLO properties.[43] The effect of proaromatic donor can be demonstrated when comparing $\mu\beta$ values of **6a** (400×10^{-48} esu) with structural analogues **1a** (330), **1b** (190) and **1e** (290) bearing *N*,*N*-dimethylamino, *N*,*N*-diphenylamino, and piperidin-1-yl donors. Further pyranylidene replacement by ferrocene (**6c**) or shortening

Accepted manuscript

the π-linker (**6a** vs. **6b**) has detrimental effect on the NLO response. As can be seen from the data gathered in Table 3, further π-linker variation/extension by introducing ferrocene (**6d**), phenyl(ethynyl)$_n$ units (**6e**, n = 1 and **6g**, n = 2), and thienyl-ethynyl (**6f**) units has also negatively affected the $\mu\beta$ values compared to parent **6a**. On the contrary, *N*-methylation of the pyrimidine ring enhanced the molecular nonlinearity of **7b**-**g** dramatically. Compared to parent **6f**, quaternized NLOphore **7f** bearing thienylethynyl π-linker possesses the NLO response more than ten-times higher. It should be mentioned that **8a,** a quadrupolar 4,6-distyryl analogue of compound **6a**, gave almost two times higher $\mu\beta$ value (770 × 10^{-48} esu).[43a]

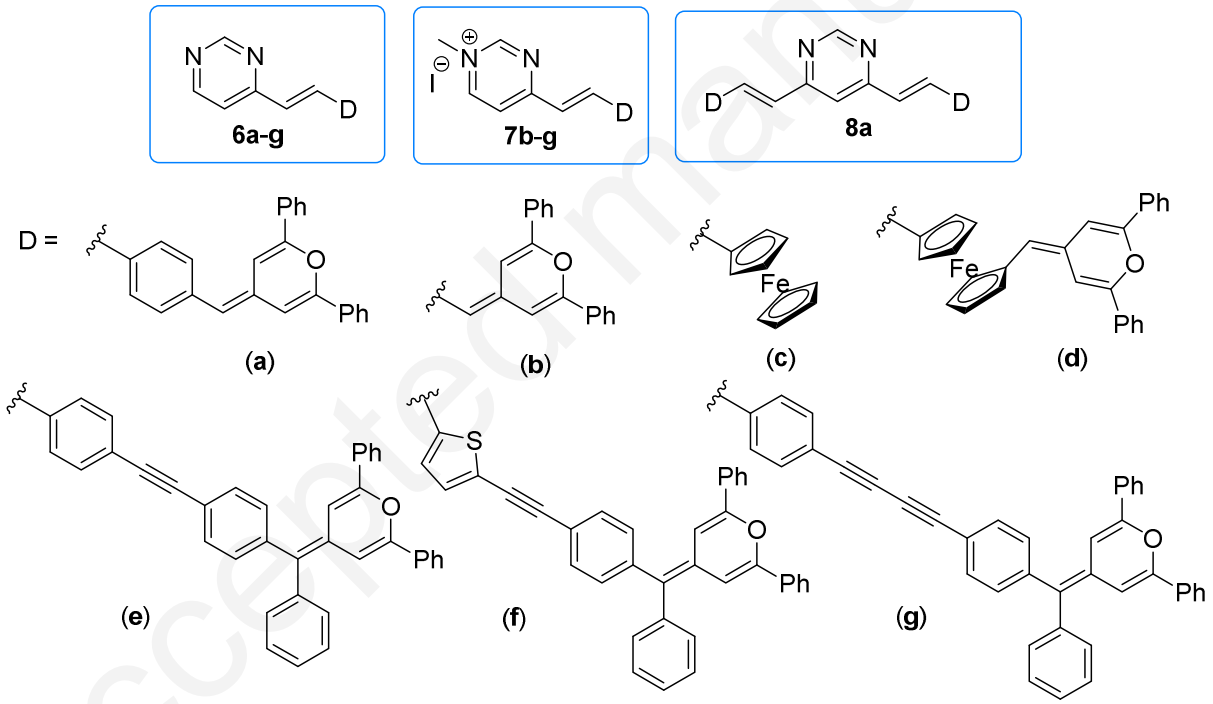


Figure 3 Pyrimidines **6–8** with proaromatic pyranylidene donor

Table 3: 2nd order NLO response of chromophores **6–8** measured by EFISH method

Compds	λ_{abs} (nm)[a]	$\mu\beta$,[b] 10^{-48} esu	$\mu\beta_0$,[c] 10^{-30} esu	Ref
6a	436	400	300	43a
6b	452	310	227	43b
6c	482	160	149	38a
6d	512	60	40	43b
6e	408	380	295	43c
6f	383	220	177	43c

Accepted manuscript

6g	410	160	120	43d
7b	624	2220	1133	43b
7c	626	< 550[d]	< 279[d]	43b
7d	684	1320	558	43b
7e	540	950	594	43c
7f	579	2300	1318	43c
7g	540	770	480	43d
8a	458	770	480	43a

[a] Measured in $CHCl_3$ (in CH_2Cl_2 for **6a**, **6c** and **8a**) [b]Measured in $CHCl_3$ at 1907 nm [c]Two level corrected β value.[14] [d] No stable $\mu\beta$ value was obtained.

Aforementioned acetylene derivatives were further used to prepare organometallic derivatives **9–12** whose structures are presented in Figure 4.[43b-d] Metal σ-acetylide fragments are generally used as electron-releasing part but $Pt(P(Tol)_3)_2$ in **9–10** and $Ru(dppe)_2$ in **11–12** were employed as a part of the π-linker. In general, an incorporation of metal σ-acetylide into the chromophore backbone results in planar arrangement, efficient coupling between the d orbitals of the metal and π^* system of the σ-acetylide bridge, pronounced ICT, and significantly increased NLO response.[44] Based on the EFISH measurements shown in Table 4, the following conclusions can be drawn: i) replacement of 1,4-phenylene by 2,5-thienylene unit (e.g. **9a**→**9b**) slightly decreases $\mu\beta$ values; ii) variation of the R-substituents (Ph vs. *t*Bu) has diminished effect on the nonlinearity, but slightly larger $\mu\beta$ values were recorded for *t*Bu derivatives (e.g. **9a/9c** or **11a/11b**); iii) central organometallic core based on ruthenium [$Ru(dppe)_2$] brings significantly higher nonlinear optical properties than $Pt(P(Tol)_3)_2$ (e.g. **9a/11a** or **10c/12b**), and iv) pyrimidine quaternization dramatically increases the measured $\mu\beta$ values (e.g. **9/10** or **11/12**). Ru-based NLOphores **12** bearing methylpyrimidinium acceptor showed exceptional NLO response of 14.000×10^{-48} esu.

Accepted manuscript

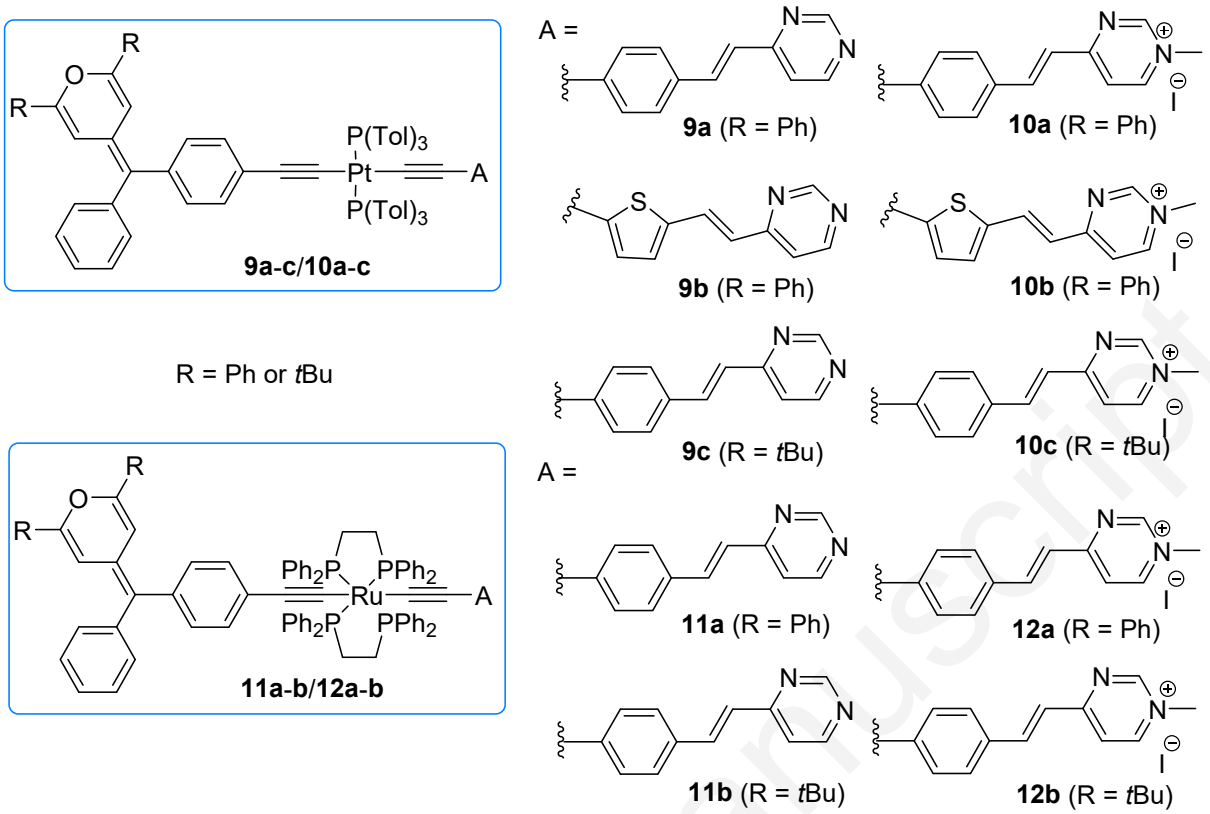


Figure 4 Organometallic pyrimidine derivatives **9–12**

Table 4: 2nd order NLO response of chromophores **9–12** measured by EFISH method

Compds	λ_{abs} (nm)[a]	$\mu\beta$,[b] 10^{-48} esu	$\mu\beta_0$,[c] 10^{-30} esu	Ref
9a	407	260	203	43c
9b	436	170	127	43c
9c	398	390	308	43c
10a	527	2000	1283	43c
10b	584	3600	2039	43c
10c	521	3600	2338	43c
11a	458	1700	1200	43d
11b	460	2200	1600	43d
12a	683	14000	5900	43d
12b	678	14000	6000	43d

[a] Measured in $CHCl_3$ [b]Measured in $CHCl_3$ at 1907 nm [c]Two level corrected β value.[14]

So far in this chapter and based on its well-known electron deficiency, the pyrimidine has been utilized as electron-withdrawing part of D-π-A systems. Recently, we have focused on incorporation of the pyrimidine ring into a π-linker as in chromophores **13** (Figure 5, Table 5).[45] Whereas the *N*,*N*-diphenylamino group was used as donor, cyclopenta[*c*]thiophen-4,6-dione (ThDione) acts as electron-acceptor; both were linked to pyrimidine core at positions 2

Accepted manuscript

and 5. Besides pyrimidine, benzene, pyridazine, and 2,5-thienylene were also employed as part of the π-backbone for comparison. The latter allowed the highest ICT from the diphenylamino donor to the ThDione acceptor. However, pyrimidine ICT transparency strongly depends on the mutual orientation of the appended donor and acceptor. Whereas linking ThDione/*N*,*N*-diphenylamine at positions 2/5 brings significant NLO response (**13a** and **13c**), the opposite arrangement has detrimental effect on the optical nonlinearity (**13b** and **13d**). It can be explained by lower μ values in these later cases. Further planarization and extension of the π-system by olefinic unit as in **13c/13d** play significant role especially in **13c** with the $\mu\beta$ value enhanced up to 410×10^{-48} esu. NLO response for 13b and 13d are rather similar and in the

Table 5: 2nd order NLO response of chromophores **13** measured by EFISH method

Compds	λ_{abs} (nm)[a]	$\mu\beta$,[b] 10^{-48} esu	$\mu\beta_0$,[c] 10^{-30} esu	Ref
13a	443	220	163	45
13b	450	70	51	45
13c	451	410	300	45
13d	459	50	36	45

[a] Measured in $CHCl_3$ [b] Measured in $CHCl_3$ at 1907 nm [c] Two level corrected β value.[14]

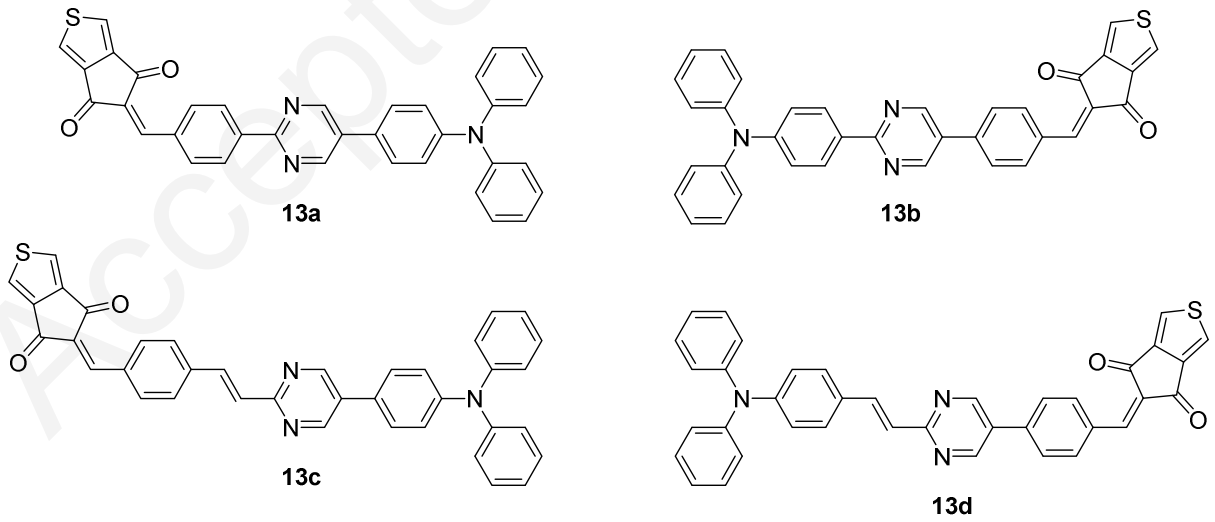


Figure 5 Pyrimidine as a part of π-conjugated linker

Accepted manuscript

It should be noted that the $\mu\beta$ of all previous compounds described in this chapter are positive indicating excited states more polarized than the ground state ($\mu_e > \mu_g$) and both states are polarized in the same direction. These positive values are in accordance with the emission solvatochromism observed for these compounds.

In 2009, He et al. reported on push-pull chromophores **14** based on 2-aminoazapyrimidines linked to 2-nitrothiazole that are easily available via azo-coupling (Figure 6).[46] Their molecular hyperpolarizabilities were investigated by HRS technique (Table 6). Considering the amino donor and nitro acceptor, pyrimidine acts as a part of the π-conjugated path similar to **13**. The replacement of the thiazole linker of compound **14a** by a phenylene one (compound **14c**) significantly reduces the NLO response. The amino group may further be *N*-substituted with hydroxyethyl to provide anchoring group.

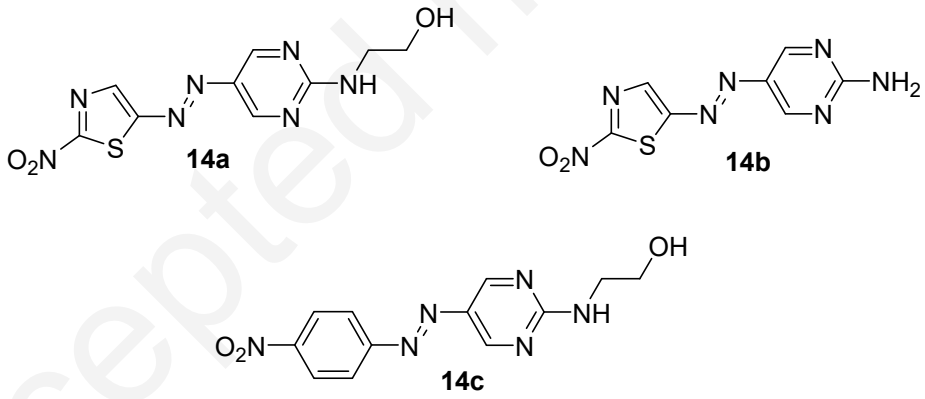


Figure 6 2-Aminopyrimidine azo derivatives **14**

Table 6: 2nd order NLO response of chromophores **14** measured by HRS technique

Compds	λ_{abs} (nm)[a]	β_{HRS},[b] 10^{-30} esu	β_0,[c] 10^{-30} esu	Ref
14a	544	510	316	46
14b	540	500	312	46
14c	475	80	56	46

[a] Measured in DMF [b] Measured in DMF at 1064 nm [c] Two level corrected β value.[14]

Accepted manuscript

2,2'-Bipyrimidine octupolar chromophores **15** bearing styryl units with amino or alkoxy electron donors are displayed in Figure 7.[47] Results of HRS/HLS measurement are given in Table 7. Noncentrosymmetric chiral derivatives **15a** are organized into left- and right-handed supramolecular aggregates/flexible thin films and allow translation of the NLO response from the molecular to the bulk level.[47b] Hence, property tuning in **15** (Table 7) can be achieved by varying the electron-releasing unit (RO *vs.* R_2N) as well as by the structure of R-pendants. NLO response of NEt_2 and NPh_2 derivatives **15g** and **15h** are similar. Bipyrimidine chromophores **15** also proved to be strongly emissive and TPA active (see TPA part).

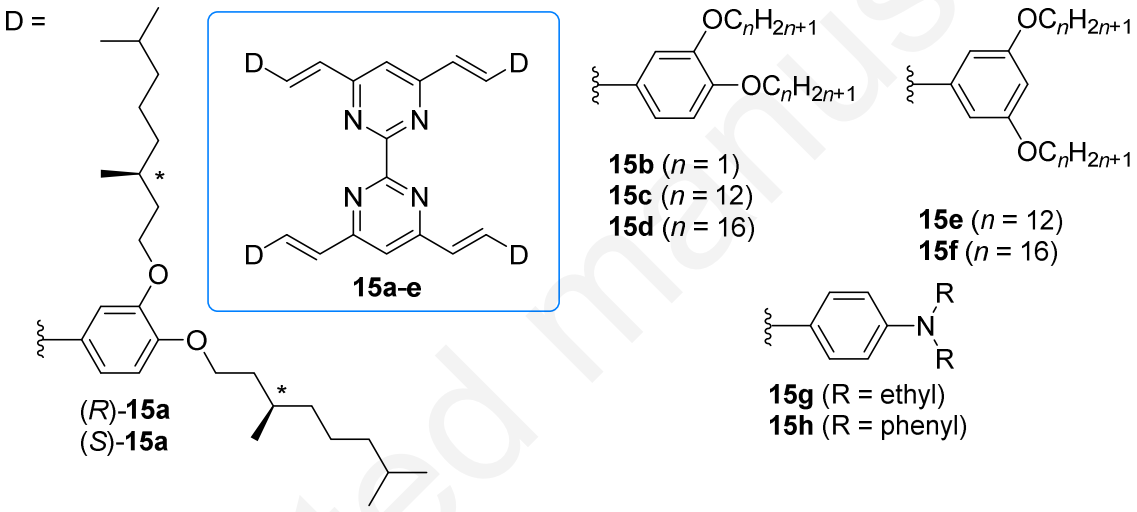


Figure 7 Bipyrimidine octupolar push-pull derivatives **15**

Table 7: 2nd order NLO response of chromophores **15** measured by HRS/HLS technique

Compds	λ_{abs} (nm)[a]	λ_{laser}(nm)	β_{HRS},[a] 10^{-30} esu	β_0,[c] 10^{-30} esu	Ref
(*R*)-**15a**	-	800	670 ± 190	48 ± 14	47a
(*S*)-**15a**	-	800	700 ± 160	66 ± 15	47a
15c	373	800	504 ± 80	38 ± 8	47b
15d	379	800	485 ± 25	42 ± 7	47b
15g	437	1640	166 ± 33[b]	110	47c
15h	421	1640	190 ± 38[b]	130	47c

[a] Measured in CH_2Cl_2, [b] HLS technique was used instead of HRS [c] Three level corrected β value for octupole

Doddamani and coworkers have described polyurethanes **P1** and **P2** incorporating a pyrimidine-based chromophore (Figure 8).[48] After corona poling, these materials exhibit SHG

Accepted manuscript

coefficient d_{33} of 95 and 86 pm/V at 532 nm. These polymers do not show any decrease of their NLO response below 100 °C and retained 95 % of their NLO response even up to 500 h. The presence of the peripheral pyrimidine fragment into the chromophores significantly enhances the NLO response.

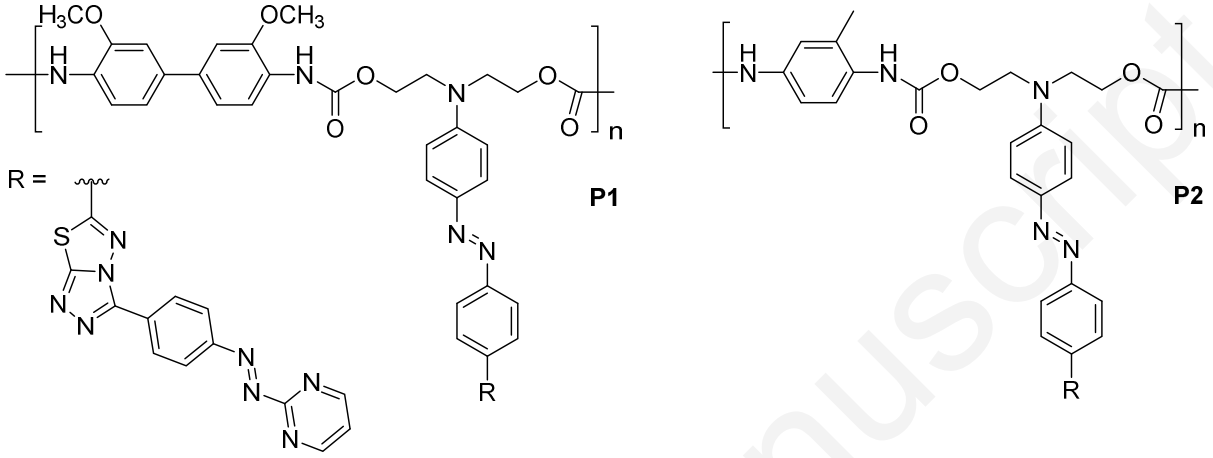


Figure 8: Structure of polyurethane polymers **P1** and **P2**

To generalize, second-order nonlinear optical properties of pyrimidine-based NLOphores are mostly influenced by the following structural features:

- strength and nature of electron-donating group: strong mesomeric and proaromatic electron releasing fragments increase the NLO response.
- length and composition of π-conjugated linker: increasing the length enhances moderately the NLO response.
- number and position of arms around the pyrimidine core: V-shaped 4,6-disubstituted pyrimidine tends to have $\mu\beta$ values more than double compared to their 4-substituted analogues.
- pyrimidine quaternization and complexation increase the NLO response very significantly
- using the pyrimidine as a π-conjugated fragment has positive effect on the NLO properties but is dependent on the ring orientation.

Accepted manuscript

3rd order NLO properties

Push-pull pyrimidine derivatives have also been extensively used as 3rd order NLOphores, mainly TPA-active molecules. These chromophores are generally based on 4- or 4,6-(di)styrylpyrimidine scaffolds. More limited studies of the real part of the $\chi^{(3)}$ of pyrimidine derivatives have been published so far.

Two-photon absorption (TPA)

In general, various structural elements can affect the TPA properties. In this chapter, we will try to highlight the effect of electron-donating substituents, π-conjugated linker, substituent on the pyrimidine core, the branching effect and the concentration of chromophores on the TPA properties of pyrimidine derivatives.

Effect of the electron donating groups

Compounds **16** with a 2-thiomethyl-4,6-distyrylpyrimidine scaffold are displayed in Figure 9.[49] Whereas methoxy and anthracenyl derivatives **16a** and **16d** exhibit low TPA cross-section, the presence of amino electron-donating groups significantly increases the TPA cross-section up to 901 GM for **16b** in MeCN due to the enhanced ICT (Table 8). The presence of a diethylamino group (**16b**) leads to significantly higher TPA cross-section than imparts dimethylamino group (**16c**, δ = 352 GM in MeCN). This can be related to the stronger electron-donating character of the diethylamino group. It should be noted that the TPA cross-sections of these compounds are largely solvent dependent.

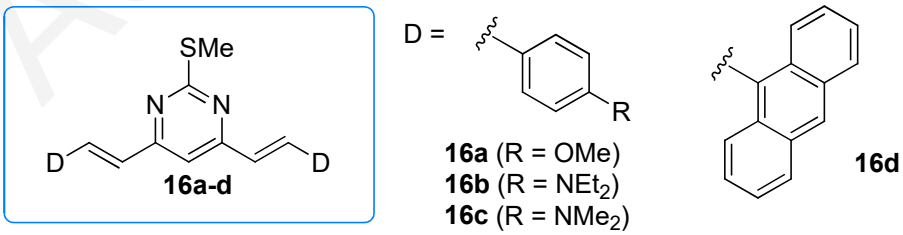


Figure 9 2-Methylthiodistyrylpyrimidines **16** with TPA activity

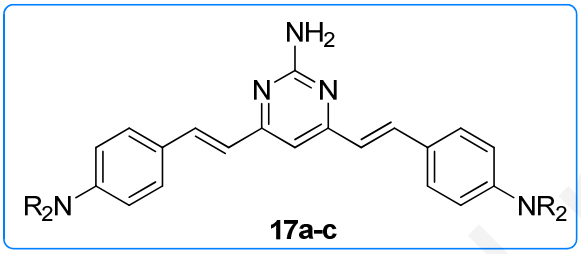
Table 8: TPA properties of methylthiodistyrylpyrimidines **16**

Accepted manuscript

Compds	Technique	Solvent	λ_{TPA} (nm)	δ(GM)	Ref
16a	TPEF	Toluene	720	5	49a
16a	TPEF	MeCN	-[a]	20	49a
16b	TPEF	Toluene	800	310	49a
16b	TPEF	MeCN	-[a]	901	49a
16c	TPEF	MeCN	800	352	49b
16d	TPEF	Toluene	740	8	49a
16d	TPEF	MeCN	-[a]	21	49a

[a] Data not available

Considering 2-amino-4,6-distyrylpyrimidine derivatives **17**, bearing diphenylamino and dialkylamino peripheral substituents (Figure 10, Table 9), the TPA cross-section increases in the following order: NMe_2 (**17a**) < NEt_2 (**17b**) < NPh_2 (**17c**).[50] Similarly to **16**, a strong solvent effect is observed; the highest cross cross-section values were measured in toluene.



17a-c

R = Me (**a**), Et (**b**), Ph (**c**)

Figure 10 2-Aminodistyrylpyrimidines **17**

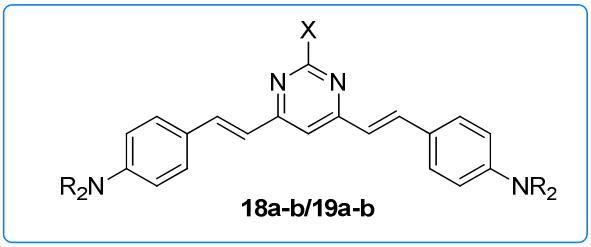
Table 9 : TPA properties of 2-mminodistyrylpyrimidines **17**

Compds	Technique	Solvent	λ_{TPA} (nm)	δ(GM)	Ref
17a	TPEF	Toluene	800	475	50
17a	TPEF	MeCN	840	366	50
17b	TPEF	Toluene	800	596	50
17b	TPEF	MeCN	840	461	50
17c	TPEF	Toluene	800	819	50
17c	TPEF	MeCN	840	625	50

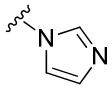
The TPA properties of compounds **18** and **19** displayed in Figure 11 indicates a strong enhancement of the TPA cross-section when the alkyl chains of the amino groups are replaced by methoxyethoxyethyl chains (Table 10). In this respect, compound **18b** (δ = 1450 GM) exhibits higher TPA cross-section than **18a** (δ = 786 GM) in MeCN. In benzene, the

Accepted manuscript

compound **19b** exhibits a TPA cross-section 1.5-times higher than that of **19a**. A higher electron donating strength of the latter donor group has been proposed to explain this increase.[51] Moreover, the methoxydiethylene glycol chains induce water solubility, a property valuable for biological imaging application.



X = Cl **18a** R = $(CH_2)_5CH_3$
18b R = $(CH_2)_2O(CH_2)_2OCH_3$

X = 

19a R = Et
19b R = $(CH_2)_2O(CH_2)_2OCH_3$

Figure 11 Distyrylpyrimidines **18** and **19** with various pendants X and peripheral donors

Table 10: TPA properties of distyrylpyrimidines **18** and **19**

Compds	Technique	Solvent	λ_{TPA} (nm)	δ(GM)	Ref
18a	TPEF	MeCN	850	786	52
18b	TPEF	MeCN	820	1450	52
19a	TPEF	Benzene	840	1890	53
19a	TPEF	MeCN	840	620	53
19b	TPEF	Benzene	840	2844	51
19b	TPEF	THF	840	3335	51

Zhang and coworker have designed a series of (diphenylaminostyryl)pyrimidine derivatives **20** and **21** displayed in Figure 12.[54] Introducing ethoxy fragments as auxiliary electron-donating group in *para* position of the phenyl rings of NPh_2 group results surprisingly in emission quenching. Nevertheless, open aperture Z-scan measurements in DMF reveal increased TPA cross-sections for compounds **20b** and **21b** compared to their unsubstituted analogues **20a** and **21a** (measured with TPEF method) (Table 11). It should however be mentioned that the TPA cross section measurement can be strongly affected by the method but also by the laser characteristics.

Accepted manuscript

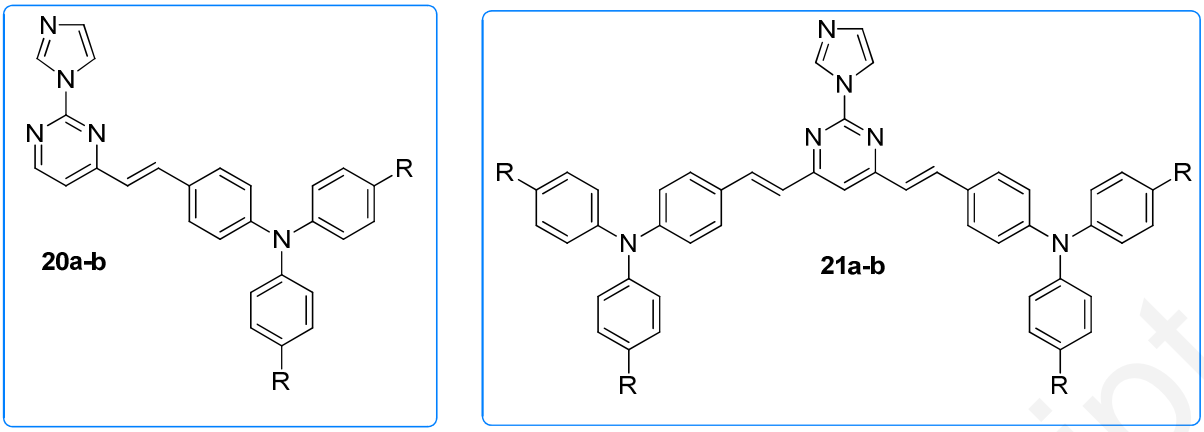


Figure 12 2-Imidazolylpyrimidines **20** and **21** with triphenylphenylamino donors

Table 11: TPA properties of 2-Imidazolylpyrimidines **20** and **21**

Compds	Technique	Solvent	λ_{TPA} (nm)	δ(GM)	Ref
20a	TPEF	DMF	890	120	54
20b	Z Scan	DMF	730	490	54
21a	TPEF	DMF	890	138	54
21b	Z Scan	DMF	820	641	54

The TPA properties of styrylpyrimidine derivatives **6a** and **8a** (Figure 3) substituted by proaromatic pyranylidene electron-donating groups have also been studied by open-aperture Z-scan technique in dichloromethane (Table 12). The TPA cross-section has been revealed in the same order as for diphenylamino analogues.[43a]

Table 11 : TPA properties of pyranylidene derivatives **6a** and **8a**

Compds	Technique	Solvent	λ_{TPA} (nm)	δ(GM)	Ref
6a	Z Scan	CH_2Cl_2	880	86	43a
8a	Z Scan	CH_2Cl_2	900	271	43a

A series of porphyrin substituted 4,6-diethynylpyrmidines **22** and **23** have been designed (Figure 13).[55] These compounds exhibit moderate TPA cross-sections but **22** possesses TPA cross-section higher than ethynylporphyrin (~20 GM).[56] Compared to other porphyrin dimers with a butadiyne linker (δ more than 5000 GM), TPA activity of **22** and **23** remains lower.[56,57] It should be noted that compound **22a** exhibits two emission bands at 648 [Q(0.0) band]

Accepted manuscript

and 702 nm [Q(0.1) band]. The data provided in Table 13 correspond to TPEF collected at 702 nm; the highest recorded cross-section is significantly lower and blue-shifted when collected at 648 nm. In case of compounds **22b–e** and **23**, the TPA was only studied at 880 nm. This wavelength corresponds to double of the Soret Band on one-photon absorption but may not correspond to the maxima of the TPA spectra, which may explain the lower cross-section compared to **22a**. No significant difference has been observed in TPA cross-section between Zn-porphyrin derivatives and their free bases.

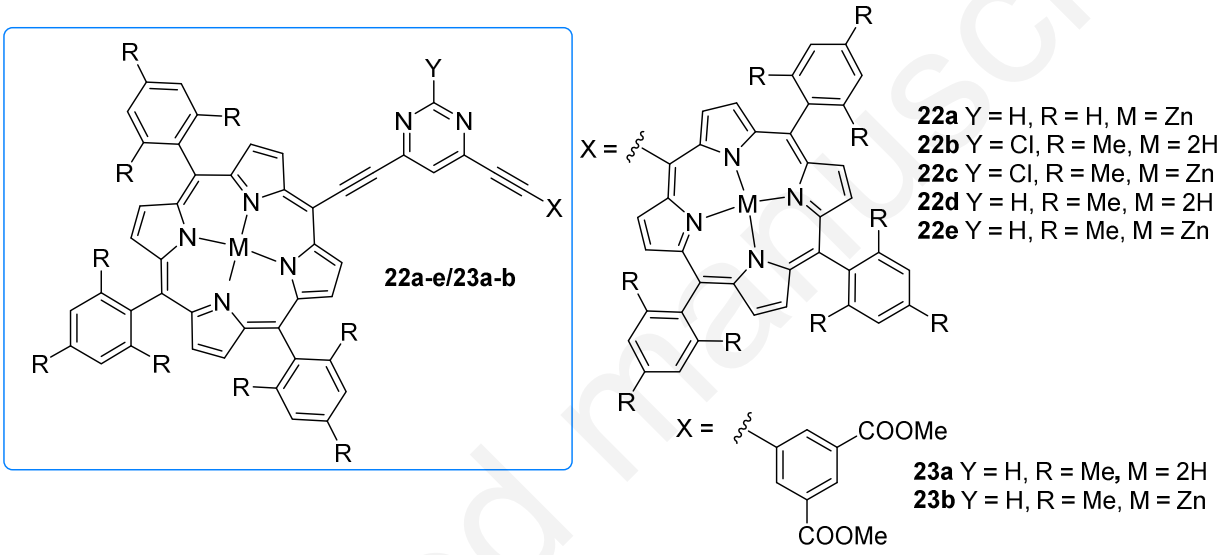


Figure 13 Ethynylpyrimidine-substituted porphyrins **22** and **23**

Table 13: TPA properties of ethynylpyrimidine-substituted porphyrins **22** and **23**

Compds	Technique	Solvent	λ_{TPA} (nm)	δ(GM)	Ref
22a	TPEF	CH_2Cl_2	930	120	55a
22b	TPEF	$CHCl_3$	880	57	55b
22c	TPEF	$CHCl_3$	880	36	55b
22d	TPEF	$CHCl_3$	880	76	55b
22e	TPEF	$CHCl_3$	880	82	55b
23a	TPEF	$CHCl_3$	880	66	55b
23b	TPEF	$CHCl_3$	880	80	55b

Effect of π-conjugated linker

Another key parameter that controls the ICT between the donor and acceptor in push-pull structure is the nature of the π-conjugated linker.[58] In this context, Chen and coworkers have

Accepted manuscript

designed 4,6-bis(thien-2-ylvinyl)pyrimidine derivatives **24** (Figure 14).[59] These compounds exhibit large cross-section values (Table 14) independently of the peripherical donor (weak for **24b**, strong for **24a**). It is unfortunately not possible to estimate the influence of the 2,5-thienylene linkers since the TPA properties of analogues compounds without these fragments are not known.

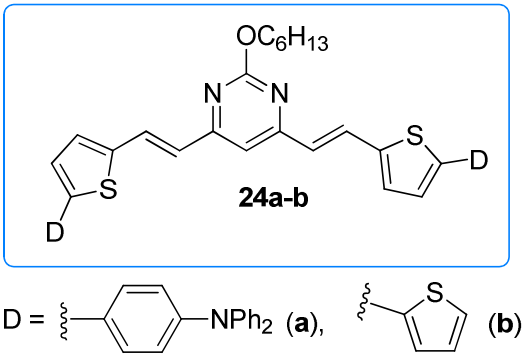
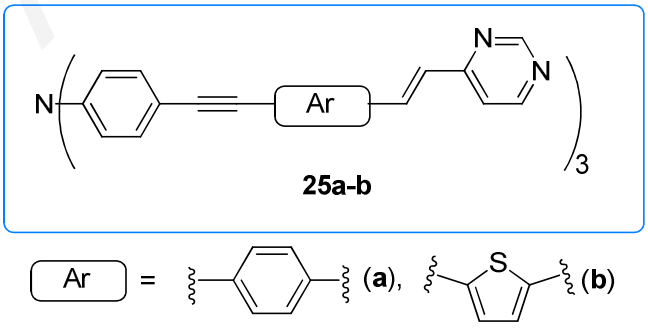


Figure 14 Structure of bis(thienylvinyl)pyrimidines **24**

Table 14: TPA properties of bis(thienylvinyl)pyrimidines **24**

Compds	Technique	Solvent	λ_{TPA} (nm)	δ(GM)	Ref
24a	TPEF	CH_2Cl_2	820	1879	59
24b	TPEF	CH_2Cl_2	810	1702	59

The comparison of 1,4-phenylene and 2,5-thienylene linkers can be done with tripodal compounds **25** bearing central triphenylamine core and pyrimidine peripheral fragments (Figure 15).[60] As expected,[40] the 2,5-thienylene linker leads to a red-shifted TPA band as well as a 1.7-increase of the cross-section in CH_2Cl_2 (Table 15). These compounds exhibit relatively moderate TPA cross-section but their fluorescence quantum yield is rather interesting (Φ > 0.5 in CH_2Cl_2).



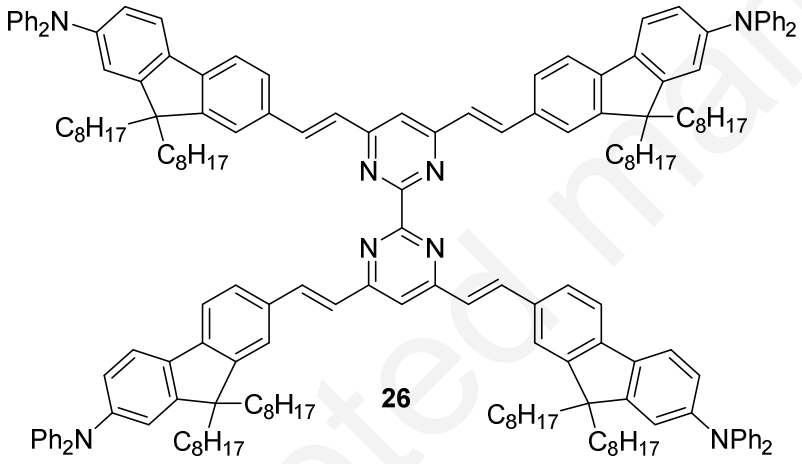
Accepted manuscript

Figure 15 Tripodal chromophores **25** based on triphenylamine core and pyrimidin-4-yl peripheral acceptors

Table 15 : TPA properties of tripodal chromophores **25**

Compds	Technique	Solvent	λ_{TPA} (nm)	δ(GM)	Ref
25a	TPEF	CH_2Cl_2	750	240	60
25b	TPEF	CH_2Cl_2	800	410	60

Bipyrimidine chromophores **15g-h** and **26** designed by Savel and coworkers (Figures 7 and 16) allow to compare 1,4-phenylene and fluorenylene π-spacer.[61] As expected due to the increased conjugated path, the fluorene derivative **26** exhibit a 2.4-higher TPA cross-section than analogue **15h** (Table 16).



26

Figure 16 Branched bipyrimidines **26**

Table 16: TPA properties of bipyrimidine chromophores **15h–g** and **26**

Compds	Technique	Solvent	λ_{TPA} (nm)	δ(GM)	Ref
15g	TPEF	$CHCl_3$	775	530	61
15h	TPEF	$CHCl_3$	790	460	61
26	TPEF	$CHCl_3$	790/860/960	1022/880/41	61

Fluorene fragments have also been incorporated in the scaffold of chromophores **27** (Figure 17).[62] In these examples, the 4,6-dimethylpyrimidin-2-yl group is used as electron-withdrawing part, while the dimethylamino group is used as electron-donating group. The TPA maxima in the red region of the spectra are slightly red-shifted concerning the double of

Accepted manuscript

one-photon absorption maxima (Table 17). Surprisingly, addition of two ethynyl linkers between the central fluorene core and the peripheral fragments leads to a significant decrease of the cross-section (**27a** *vs.* **27b**). On the contrary, replacement of only one triple bond by a triazole unit on the pyrimidine side (compound **27c**) increases the TPA cross-section up to 148 GM. When two triazole rings are present on each side of the fluorene (compound **27d**), the cross-section is dramatically decreased and the TPA maxima is blue shifted.

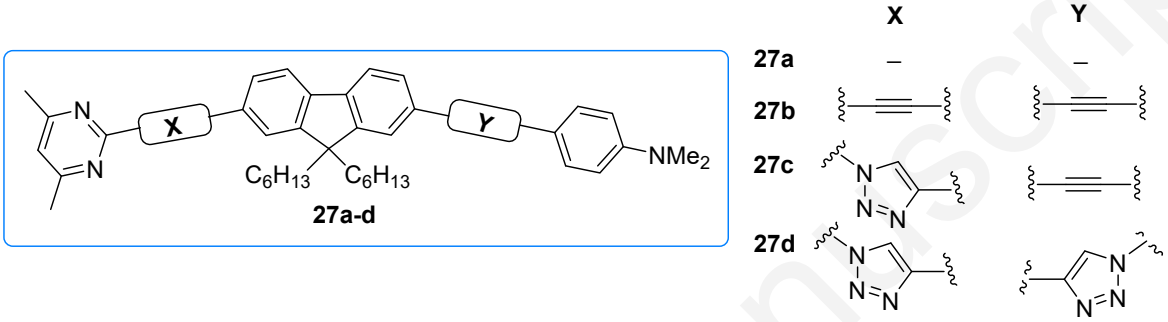


Figure 17: Fluorene-based chromophores **27**

Table 17: TPA properties of fluorene-based chromophores **27**

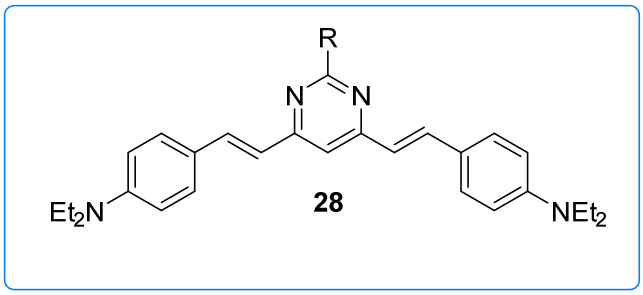
Compds	Technique	Solvent	λ_{TPA} (nm)	δ(GM)	Ref
27a	TPEF	CH_2Cl_2	740	123	62
27b	TPEF	CH_2Cl_2	760	82	62
27c	TPEF	CH_2Cl_2	760	148	62
27d	TPEF	CH_2Cl_2	700	39	62

Influence of the C2 substituent on the pyrimidine core

As seen before, the majority of the pyrimidine chromophores are based on the 4,6-distyrylpyrimidine moiety. In these chromophores, the substituent in C2 position of the pyrimidine core can significantly affect the photophysical properties including TPA. Liu and coworkers have designed a series of 4,6-bis(*N*,*N*-diethylanimostyryl)pyrimidine derivatives **28a-f** with various substituents in C2 position (Figure 18).[63] The electron-donating substituent in the C2 position such as a *p*-*N*,*N*-dimethylaminophenyl group (compound **28a**) tends to decrease the TPA cross-section. On the other hand, electron-withdrawing fragment such as *p*-cyanophenyl (compound **28e**) or a pyridin-4-yl (compound **28f**) significantly enhances the

Accepted manuscript

TPA cross-section up to 720 GM in $CHCl_3$ (Table 18). The pyrazol-1-yl derivative **28h** exhibits cross-section significantly lower than imidazol-1-yl and thiophen-2-yl analogues **19a** and **28g** (Figures 11 and 18, Tables 10 and 18).[53,64] The TPA cross-section of the latter measured with Z-scan method was significantly higher than with TPEF method. The authors admitted that this value is probably overestimated. This illustrates the difficulties to properly compare data obtained by different methods.



28a R = *p*-C_6H_4-NMe_2
28b R = *p*-C_6H_4-OMe
28c R = *p*-C_6H_4-Me
28d R = Ph
28e R = *p*-C_6H_4-CN
28f R = pyridin-2-yl
28g R = thiophen-2-yl
28h R = pyrazol-1-yl

Figure 18: Structure of 2-substituted 4,6-bis(*N*,*N*-diethylaminostyryl)pyrimidines **28**

Table 18: TPA properties of 4,6-bis(*N*,*N*-diethylaminostyryl)pyrimidines **28**

Compds	Technique	Solvent	λ_{TPA} (nm)	δ(GM)	Ref
28a	TPEF	$CHCl_3$	820	340	63
28b	TPEF	$CHCl_3$	820	390	63
28c	TPEF	$CHCl_3$	820	390	63
28d	TPEF	$CHCl_3$	820	400	63
28e	TPEF	$CHCl_3$	810	720	63
28f	TPEF	$CHCl_3$	810	624	63
28g	TPEF	CH_2Cl_2	840	600	64
28g	TPEF	MeCN	840	2000	64
28g	Z Scan	CH_2Cl_2	780	19125	64
28h	TPEF	Benzene	830	660	53
28h	TPEF	MeCN	830	180	53

Yang and coworkers have designed chromophores **29** (Figure 19) for bioimaging application.[65] The isocyanate group in compound **29a** is intended for coupling with the amino group of a biomolecule. Compound **29b** bearing a D-glucosamine pendant in the C2 position of the pyrimidine core, exhibits a TPA cross-section slightly lower (337 GM) than that of the parent isocyanate precursor **29a** (512 GM, Table 19).

Accepted manuscript

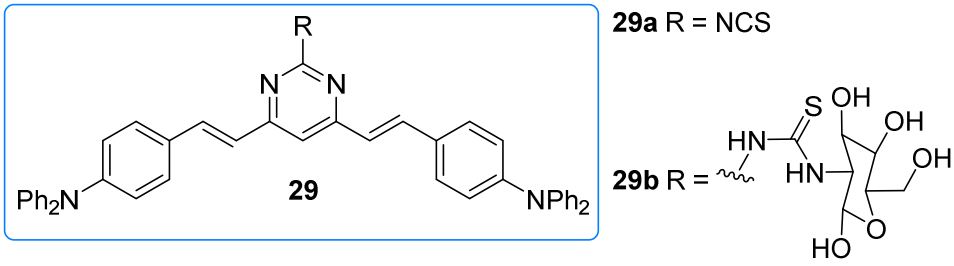


Figure 19: Distyrylpirimidines **29** for bioimaging

Table 19 : TPA properties of distyrylpirimidines **29**

Compds	Technique	Solvent	λ_{TPA} (nm)	δ(GM)	Ref
29a	TPEF	CH_2Cl_2	820	512	65
29b	TPEF	CH_2Cl_2	810	337	65

Branching effect

As presented in the introduction, a cooperative enhancement of TPA is generally observed in multi-branched structures. This is also the case of 4,6-distyrylpyrimidines that exhibit higher TPA cross-section, which is generally more than double of the corresponding 4-styrylpyrimidine analogues. For example chromophore **8a** showed TPA cross-section of 271 GM, 3.2-times higher than that of 4-styryl analogue **6a** (Figure 3, Table 11).[43a] Similarly, chromophore **16b** and **19b** exhibit significantly higher TPA cross-section than their monostyryl analogue **30a** and **30b** (Figure 21).[49a,51] Distyryl derivatives **21** possess also higher TPA cross-section than compounds **20**, despite the cooperative branching effect seems to be lower in this case (Figure 11, Table 10).[54] A comparison of compounds **31**-**33** displayed in Figure 21, confirms the significant enhancement of the TPA cross-section when going from mono to distyryl derivatives (Table 20).[66] Incorporation of a third branch in the C2 position of the pyrimidine core (compounds **33**) does not lead to C3 symmetry system and cannot be considered as real octupole. Nevertheless, an enhancement of the TPA response up to 492 GM has been observed for **33b** whereas the spectral position of TPA is maintained with regards to distyryl analogues **32**.

Accepted manuscript

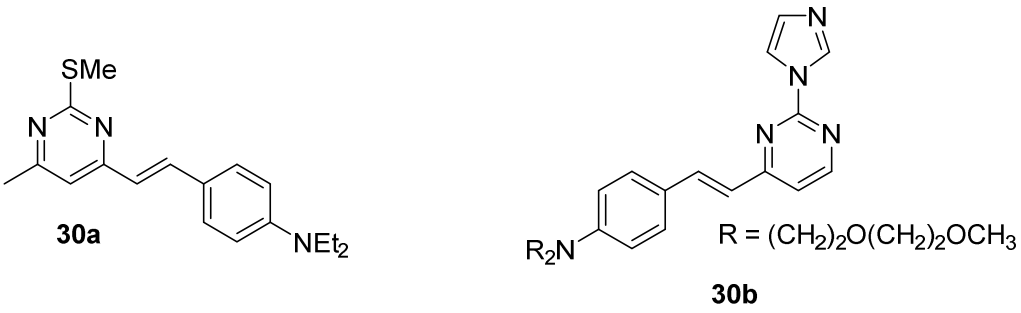


Figure 20 : Monostyryl-substituted chromophores **30**

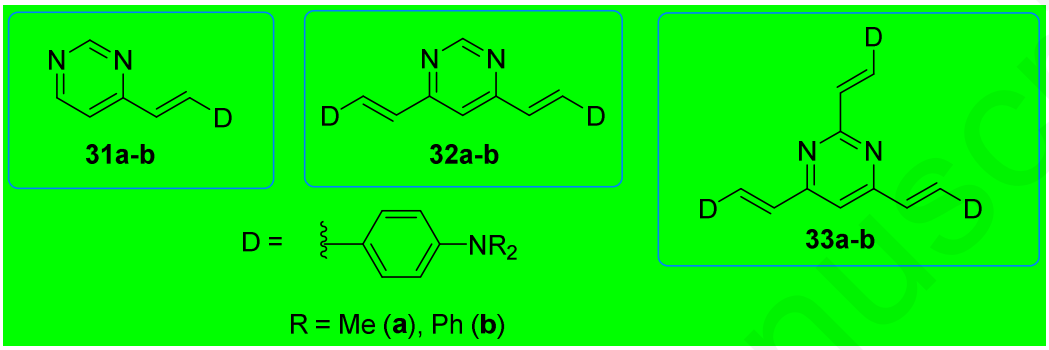


Figure 21: Mono, di and tristyryl chromophores **31–33**

Table 20: TPA properties of chromophores **30-33**

Compds	Technique	Solvent	λ_{TPA} (nm)	δ(GM)	Ref
30a	TPEF	Toluene	-	16	49a
30a	TPEF	MeCN	-	83	49a
30b	TPEF	Benzene	840	842	51
30b	TPEF	THF	860	1273	51
31a	TPEF	CH_2Cl_2	795	73	66
31b	TPEF	CH_2Cl_2	795	109	66
32a	TPEF	CH_2Cl_2	790	235	66
32b	TPEF	CH_2Cl_2	790	387	66
33a	TPEF	CH_2Cl_2	775	324	66
33b	TPEF	CH_2Cl_2	775	492	66

The cooperative branching effect on the TPA cross-section of distyrylpyrimidines can further be demonstrated on compounds **34–35**, measured by either TPEF or Z-scan techniques (Figure 22, Table 21).[67] Hexabranched molecule **36** exhibits higher TPA cross-section than **35** (870 GM in DMF with TPEF method), however its figure of merit (TPA cross-section per molecular weight) is lower.

Accepted manuscript

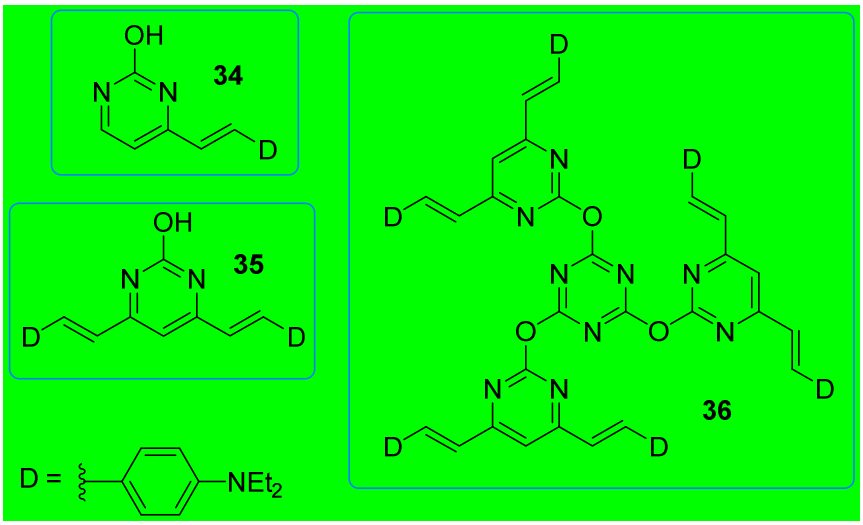


Figure 22: Multibranched structures of compounds **34–36**

Table 21: TPA properties of chromophores **34–36**

Compds	Technique	Solvent	λ_{TPA} (nm)	δ(GM)	Ref
34	TPEF	DMF	-	151	67
34	Z Scan	DMF	830	350	67
35	TPEF	DMF	840	1319	67
35	Z Scan	DMF	750	1000	67
36	TPEF	DMF	870	1885	67
36	Z Scan	DMF	750	1000	67

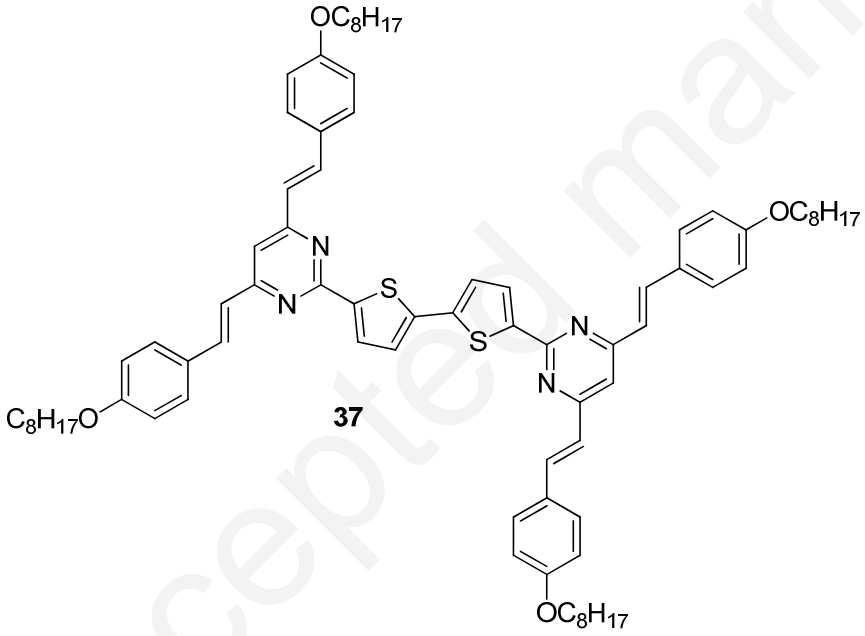
The TPA properties of 3-dimensional octupolar structures **15b-h** (Figure 7) were studied in CH_2Cl_2 (Tables 16 and 22)[47b,60] providing interesting TPA properties. When comparing octupolar bipyrimidine structure **15h** with its quadrupolar compound **32b**, an enhancement of the TPA cross-section can be noticed, which is, however, less than doubled. The complexation of compounds **15g-h** with $ZnCl_2$ induces a red shift of the TPA band and a decrease of the cross-section by a factor of 1.5 and 1.6, respectively. The complexes maintain a centrosymmetric character but the loss of three-dimensionality caused by their planarization has detrimental effect on the TPA response. In the case of **26** (Figure 16), its Zn complex maintains a 3D octupolar structure, which is attributed to the steric hindrance of the fluorenylvinylene branches as shown by DFT calculation.[68] This leads to a strong enhancement of the TPA cross-section upon complexation (Table 16 and 22).

Accepted manuscript

Table 22 : TPA properties of bipyrimidines **15b-f** and Zn complexes of bipyrimidines **15g-h** and **26.**

Compds	Technique	Solvent	λ_{TPA} (nm)	δ(GM)	Ref
15b	TPEF	CH_2Cl_2	705	325	47b
15c	TPEF	CH_2Cl_2	720	380	47b
15d	TPEF	CH_2Cl_2	705	372	47b
15e	TPEF	CH_2Cl_2	690	118	47b
15f	TPEF	CH_2Cl_2	680	113	47b
Zn15g	TPEF	CH_2Cl_2	820	353	61
Zn15h	TPEF	CH_2Cl_2	840	280	61
Zn26	TPEF	CH_2Cl_2	800/870/980	733/19996/774	61

Chen *et al.* have described another 2D multibranched conjugated system **37** depicted in Figure 23.[69] The observed TPA cross-section in DMF (1352 GM) is similar to other bipyrimidine-based multibranched structure with strong amino donor such as **15g-h**.



37

Figure 23 : Dipyrimidine bithiophene multibranched system **37**

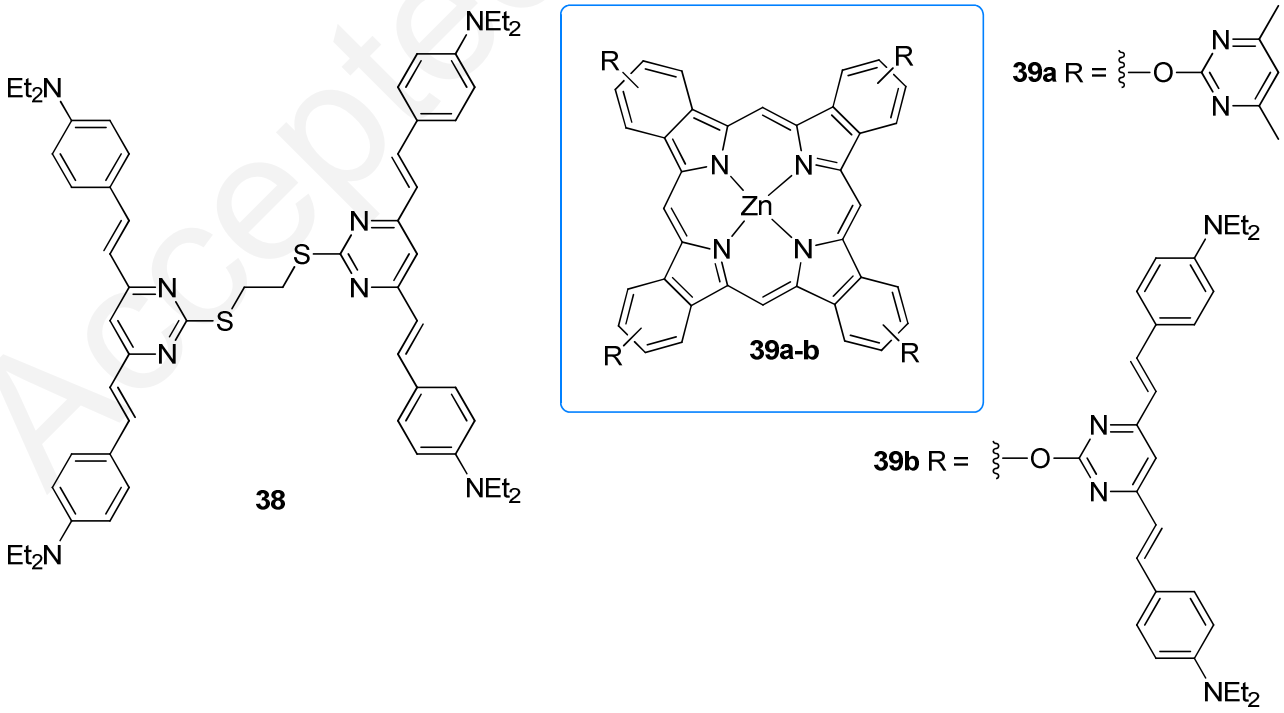
Table 23 : TPA properties of dipyrimidine bithiophene multibranched system **37**

Compds	Technique	Solvent	λ_{TPA} (nm)	δ(GM)	Ref
37	TPEF	THF	690	1352	69

Pyrimidine multicore and oligomeric systems

Accepted manuscript

Another strategy to obtain a media with high TPA cross-section involves enriching the chromophore by more pyrimidine cores or arranging the chromophore either as a nanoparticle or an oligomeric structure.[70] In the structure of chromophore **38** (Figure 24), two 4,6-distyrylpyrimidine units are linked by a non-conjugated spacer.[49a] Surprisingly, this compound exhibits a TPA cross-section in toluene that is 7-times higher than the distyrylpyrimidine parent analogue **16b**. Liu and coworkers have designed two phthalocyanine derivatives **39** bearing four pyrimidine fragments (Figure 24).[71] As expected, the chromophore bearing the distyrylpyrimidine fragments (**39b**) exhibit significantly higher TPA response than the phthalocyanine bearing dimethylpyrimidine moieties (**39a**) (Table 24). Nevertheless, the phthalocyanine core does not seem to enhance the cross-section, which is not higher than four independent 4,6-distyrylpyrimidine fragments. The beneficial effect of more pyrimidine cores can also be demonstrated by aforementioned triazine-based chromophore **36** (Figure 22), which possesses TPA cross-section up to 1885 GM (Table 21).



Accepted manuscript

Figure 24: Pyrimidine multicore systems **38** and **39**.

Table 24: TPA properties of pyrimidine multicore systems **38** and **39**.

Compds	Technique	Solvent	λ_{TPA} (nm)	δ(GM)	Ref
38	TPEF	Toluene	840	2280	49a
38	TPEF	MeCN	-	1890	49a
39a	Z Scan	DMF	830	377	71
39b	Z Scan	DMF	870	1153	71

Li *et al.* have designed dye-concentrated nanoparticles (DCNs) **40** giving rise to a large enhancement in TPA properties (Figure 25).[72] Surprisingly, the authors observed negligible TPA cross-section for the free dye in the 720-860 nm region and claimed a significant increase of the cross-section for the dye-concentrated nanoparticles (δ = 284 GM) in DMF (Table 25). Malval and coworkers have designed a conjugated copolymer **41** alternating 4,6-divinylpyrimidine and triphenylamine part comprising 8 to 10 repeating units.[73] This compound showed a helical structure leading to a weak interchromophore coupling within the oligomer. A significant cooperative enhancement with exceptional TPA activity (δ = 5093 GM) has been recorded.

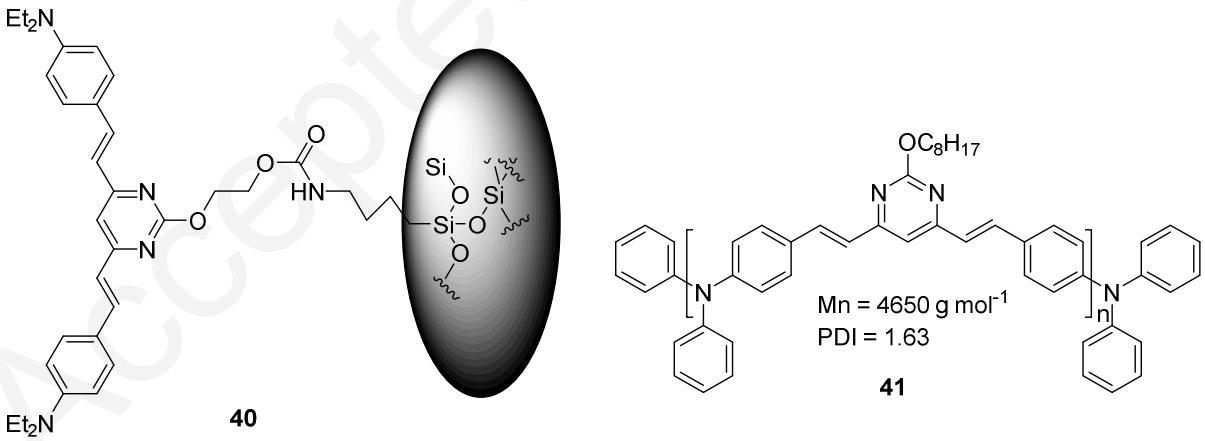


Figure 25: Structure of system **40** and **41**

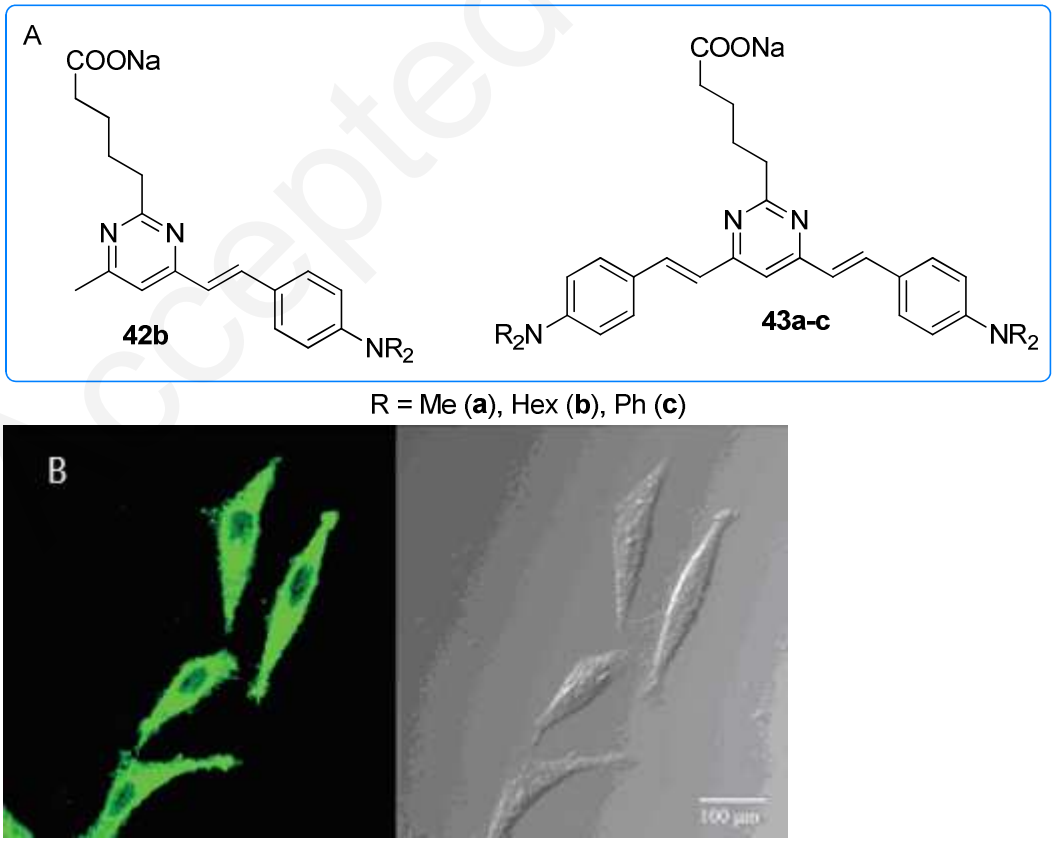
Table 25: TPA properties of chromophores **40** and **41**

Compds	Technique	Solvent	λ_{TPA} (nm)	δ(GM)	Ref
40	TPEF	DMF	830	284	72
41	TPEF	CH_2Cl_2	800	5093	73

Accepted manuscript

Application of 2PA properties of pyrimidine chromophores

The main application of pyrimidine TPA chromophores involves fluorescence microscopy imaging, which requires water-solubility. In this context, Liu and coworkers have designed a series of amphiphilic 4,6-distyrylpyrimidine derivatives **42** and **43** (Figure 26A) decorated with peripheral carboxylates.[74] Single and two-photon fluorescence microscopy imaging experiments revealed that these compounds can effectively stain the cytoplasmic region of Hep-G2 cells (Figure 26B). Similarly, the chromophores **19b**, **28g**, **29b**, **35** and the conjugate of **29a** with transferring protein can be used as cytoplasmic stainer for two-photon microscopy.[51,53,64,65,67] Compounds **44** (Figure 27), with hexafluorophosphate water-solubilizing groups have also been used for two-photon fluorescence microscopy and possess high specificity for mitochondria.[75] The chromophore **45** (Figure 27), exhibiting TPA cross-section of 39 GM at 820 nm in water/DMSO mixture, effectively targets the endoplasmic reticulum in living cells.[76] Very similar results were observed with chromophores **20a** and **21a**.[54]



Accepted manuscript

Figure 26: (A) Structure of compounds **42** and **43**. (B) Differential interference contrast (right) and two-photon microscopy image (left) of Hep-G2 cells stained with **43b**. Reproduced with permission from reference [74] (copyright 2007 Royal Chemical Society)

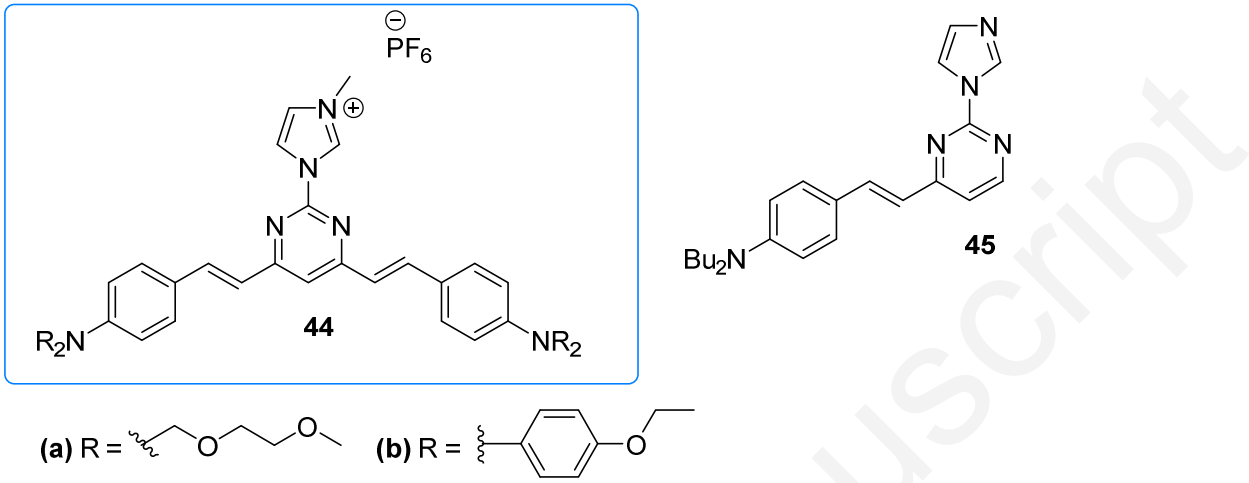
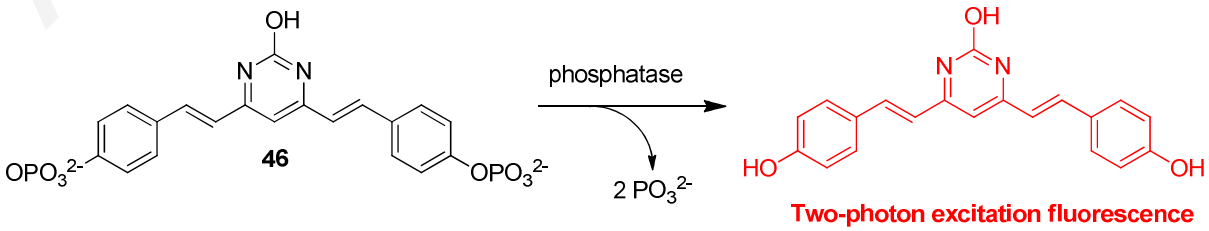


Figure 27: Pyrimidine dyes used for fluorescence microscopy bioimaging

Compound **30a** has been used for biological copper(II) detection.[77] In the presence of Cu(II), **30a** showed 2.1-fold increase of its cross-section up to 591 GM in MeCN/water (λ_{ex} = 830 nm, Z-scan measurement) associated with fluorescence quenching.

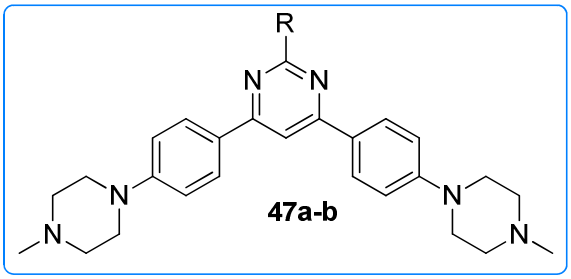
Li and coworkers have developed a system based on 4,6-distyrylpyrimidine **46** used as two-photon fluorogenic probes capable to monitor phosphatase activity in cells and tissues (Scheme 1).[78] This chromophore can be conjugated to different cell-penetrating peptides to achieve organelle- and tumor cell-specific imaging of phosphatase activities in both live mammalian cells and Drosophila brains.



Scheme 1 Distyrylpyrimidine **46** used to monitor phosphatase activity

Accepted manuscript

Compounds **47** (Figure 28) were designed as DNA fluorescent binders.[79] In both cases, a TPA cross-section enhancement up to 13.6-fold is observed in the presence of DNA due to a groove binding mechanism.



R = H (**a**), OH (**b**)

Figure 28 : DNA fluorescent binders **47**

Data recording experiments with compound **16b** proved its potential for optical data storage.[49a,80] The oligomer **41** has been used to improve the two-photon induced polymerization efficiency of a bicomponent photoinitiator system implying a hexaarylbiimidazole used as a H-abstractor and an aliphatic amine used as H-donor.[73] Pyrimidine chromophores **48** and **49** with porphyrin and ferrocene moieties have revealed to exhibit optical power limiting properties (Figure 29).[81]

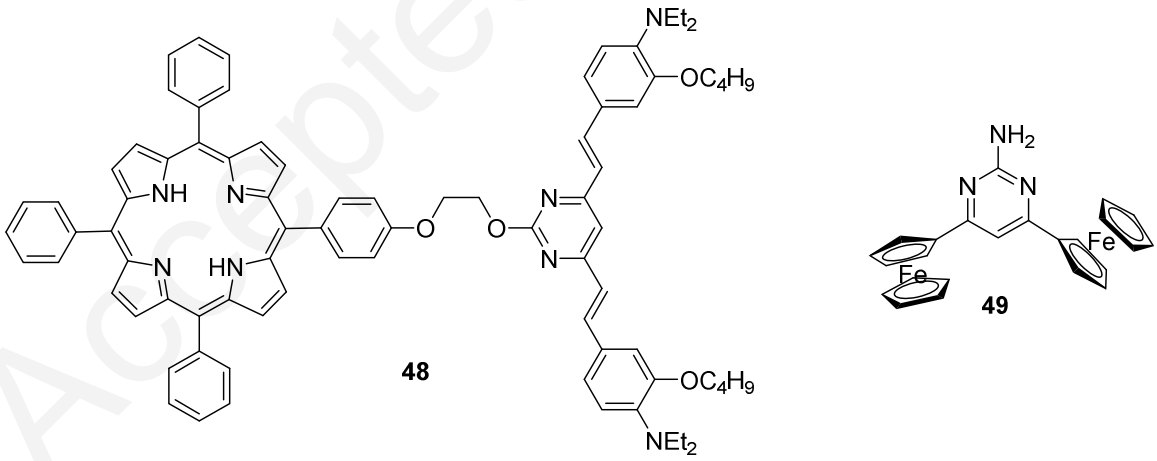


Figure 29: Pyrimidine chromophores **48** and **49** with optical power limiting properties

Other 3rd order NLO properties

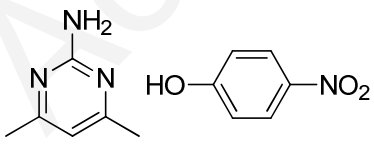
As mentioned before, the nonlinear refractive index γ can be measured by the close aperture Z-scan technique. Combined with open aperture Z-scan technique, the real *Re* and imaginary

Accepted manuscript

part *Im* as well as the effective value of the third-order NLO susceptibility $\chi^{(3)}$ can be obtained.[82] In general, tuning the *Re*/*Im* ratio is rather complicated and no clear structural guidelines have been established so far. Only few examples of pyrimidine chromophores have been investigated for their third-order NLO susceptibility γ (Table 26) and, therefore, it is rather less-straightforward to comment on structure-property relationships. When comparing ethoxy-substituted triphenylamine derivatives **20b** and **21b**, the monostyrylpyrimidine **20b** exhibits a higher value of the real part of $\chi^{(3)}$ than its 4,6-distyryl analogue **21b**.[54] For the ferrocene derivative **49**, the absolute value of the real part of $\chi^{(3)}$ is 8-times higher than its imaginary part.[81b] In case of **48**, Z-scan experiments revealed appreciable NLO refraction in addition to the NLO absorption, but no quantitative values were provided. Recently, Z-scan measurement of a co-crystal of 2-amino-4,6-dimethlypyrimidine with 4-nitrophenol **50** (Figure 30) was reported revealing an effective value of third order susceptibility of 2.48×10^{-8} esu.[83]

Table 26: Third-order NLO data for compounds **20b**, **21b**, **28g**, **49** and **50** obtained by Z-scan measurements.

Compds	Solvent	λ_{ex} (nm)	γ (m^2 W^{-1})	*Re* (10^{-8} *esu*)	*Im* (10^{-8} *esu*)	$\chi^{(3)}$ (10^{-8} esu)	Ref
20b	DMF	730	$8.21\ 10^{-9}$	4.26	3.36	5.42	53
21b	DMF	820	$2.23\ 10^{-9}$	1.16	4.19	4.35	53
58g	DMF	780	$6.69\ 10^{-16}$	$3.47\ 10^{-6}$	1.45	1.45	63
49	DMF	920	$-3.35\ 10^{-14}$	-1.74	0.218	1.75	80b
50	crystal	532				2.48	83



50

Figure 30: Structure of co-crystal **50**

Conclusion

Accepted manuscript

In summary, the pyrimidine heterocycle appears as a wonderful platform for the construction of NLO chromophores. In particular methylpyrimidinium push-pull derivatives, that can be easily obtained in a gram scale, seem to be promising material for optical data processing. Organometallic methylpyrimidinium chromophores incorporating ruthenium fragment within the π-conjugated spacer are among the best metal-diyne NLO chromophores. The 4,6-distyrylpyrimidine moiety is now a well-established TPA chromophore with advanced applications, especially for two-photon fluorescence microscopy. The pyrimidine C2 position offers a unique possibility to link various biomolecules. The resulting systems are very promising probes for biosensing of cancer cells or neurodegenerative tissues. In this context, the development of pyrimidine chromophores bearing bioorganic fragments specifically targeting these cells and tissues is probably the key points in the future of this field.

Acknowledgements

M. F. acknowledges the Région Bretagne, France, for her Ph.D. funding (HOLED project)

References

[1] (a) Göppert, M. Über die wahrscheinlichkeit des Zusammenwirkens zweier Lichtquanten in einem elementarakt. *Naturwissenchaften*, **1929**, *17*, 932-932; (b) Göppert-Mayer, M. Über elementarakte mit zwei quatensprügen *Ann. Phys.* **1931**, *401*, 273-294.

[2] Franken, P. A.; Hill, A. E;; Peters, C. W.; Weinreich, G. Generation of optical harmonics. *Phys. Rev. Lett.* **1961**, *7*, 118-119.

[3] Kaiser, W.; Garrett, C. G. B. Two-photon excitation in CaF_2:Eu^{2+} *Phys. Rev. Lett.* **1961**, *7*, 229-231.

[4] Terhune, R. W.; Maker, P. D.; Savage, C. M. Optical generation in calcite. *Phys. Rev. Lett.* **1962**, *8*, 404-406.

Accepted manuscript

[5] Boyd R. W. in Nonlinear Optics (Third Edition), Academic Press, Burlington, **2008**, pp 1-67

[6] (a) Prasad, P. N. Nonlinear Optical Properties of Organic Matrials, Plenum, New York, **1991**; (b) Bosshard, C.; Hulliger, J.; Florsheimer, M.; Gunter, P. Organic Nonlinear Optical Materials CRC Press, **2001**; (c) Nalwa, H. S.; Miyata, S. Eds., Nonlinear optics or organic molecules and polymers, CRC Press, Boca Raton, Fla, **1997.**

[7] Morita, A. Theory of sum frequency generation spectroscopy Springer Nature Singapore Pte Ltd. **2018**.

[8] Bass, M.; Franken, P. A.; Ward, J. F.; Weinreich, G. Optical Rectification, *Phys. Rev. Lett.* **1962**, *9*, 446.

[9] Blu-ray Disc Association. White Paper Blu-Ray Disc Format- Physical Format Specifications for BD-ROM, **2010**; pp 1-48.

[10] (a) Koos, C.; Vorreau, P.; Vallaitis, T.; Dumon, P.; Bogaets, W.; Baets, R.; Esembeson, B.; Biaggio, I.; Michinobu, T.; Diederich, F.; Freude, W.; Leuthold, J. All-optical high-speed signal processing with silicon-organic hybrid slot waveguides *Nat. Photonics*, **2009**, *3*, 216-219: (b) Cotter, D.; Manning, R. J.; Blow, K. J.. Ellis, A. D.; Kelly, A. E.; Nesset, D.; Phillips, I. D.; Poustie, A. J.; Rogers, D. C. Nonlinear optics for high-speed digital information processing, *Science*, **1999**, *286*, 1523-1528; (c) Jalali, B.; Fathpour, S. Silicon photonics, J. *Litghwave Techn.* **2006**, *24*, 4600-4615.

[11] (a) Dubreuil, M.; Rivet, S.; Le Grand Y. Snapshot second-harmonic generation polarimeter based on psectral analysis *Opt. Lett.*, **2017**, *42*, 4639-4642; (b) Chen. X.; Nadiarynkh, O.; Plotnikov, S.; Campagnola, P. J. Second harmonic generation microscopy for quantitative analysis of collagen fibrillar structure. *Nat. Protoc.*, **2012**, *7*, 654-669; (c) Campagnola, P. J.; Loew, L. M. Second-harmonic imaging microscopy for visualizing biomolecular arrys in cells, tissues and organisms. *Nat. Biotechn.*, **2003**, *21*, 1356-1360

Accepted manuscript

[12] Zyss, J.; Ledoux, I.; Nonlinear optics in multipolar media – theory and experiments. Chem. *Rev.*, **1994**, *94*, 77-105.

[13] Terhune, R. W.; Maker, P. D.; Savage, C. M. Measurements of nonlinear light scattering *Phys. Rev. Lett.*, **1965**, *61*, 681-684

[14] (a) Oudar, J. L.; Chemla, D. S. Hyperpolarizabilities of the nitroanilines and their relations to the excited state dipole moment *J. Chem. Phys.* **1977**, *66*, 2664-2668 ; (b) Kanis, D. R.; Ratner, M. A.; Marks, T. J. Design and construction of molecular assemblies with large second order optical nonlinearities. Quantum chemical aspects. *Chem. Rev.* **1994**, *94*, 195-242.

[15] Dalton, L. R.; Sullivan, P. A.; Bale, D. H. Electric field poled organic electro-optic materials: state of the art and future prospects. *Chem. Rev.*, **2010**, *110*, 25-55.

[16] (a) He, G. S.; Tan, L.-S.; Zheng, Q.; Prasad, P. N. Multiphoton absorbing materials: molecular design, characterizations and applications. *Chem. Rev.*, **2008**, *108*, 1245-1330; (b) Pawlicki, M.; Collins, H. A.; Denning, R. G.; Anderson, H. L. Two-photon aabsorption and the design of two-photon dyes. *Angew. Chem. Int. Ed.*, **2009**, *48*, 3244-3266.

[17] (a) Cao, L.; Wang, X.; Meziani, M. J.; Lu, F. S.; Wang, H. F.; Luo, P. J. G.; Lin, Y.; Harruff, B. A.; Veca, L. M.; Murray, D.; Xie, S.-Y.; Sun, Y.-P. Carbon dots for multiphoton bioimaging. *J. Am. Chem. Soc.* **2007**, *129*, 11318-11319; (b) Xu, C.; Zipfel, W.; Shear, J. B.; Williams, R. M.; Webb, W. W. Multiphoton fluorescence excitation: new spectral windows for biological nonlinear microscopy. *Proc.Natl. Acad. Sci. U.S.A.***1996**, *93*, 10763-10768; (c) Helmchen, F.; Denk, W. Deep tissue two-photon microscopy. *Nat. Methods*, **2005**, *2*, 932-940.

[18] (a) Kawata, S.; Sun, H. B.; Tanaka, T.; Takada, K. Finer features for functional microdevices – Micromachines can be created with higher resolution using two-photon absorption. *Nature*, **2001**, *412*, 697-698; (b) Wang, I.; Bouriau, M. Baldeck, P. L.; Martineau,

Accepted manuscript

C.; Andraud, C. Three-dimentional microfabrication by two-photon-initiated polymerization with a low-cost microlaser. *Opt. Lett.*, **2002**, *27*, 1348-1350; (c) Xia, R.; Malval, J.-P.; Jin, M.; Spangenberg, A.; Wan, D.; Pu, H.; Vergote, T.; Morlet-Savary, F.; Chaumeil, H.; Baldeck, P.; Poizat, O.; Soppera, O.; Chem. Mater. Enhancement of acid photogeneration through a para-to-meta substitution strategy in a sulfonium-based alkoxystilbene designed from two-photon polymerization *Chem. Mater.*, **2012**, *24*, 237-244.

[19] (a) Morel, Y.; Irimia, A.; Najechalski, P.; Kervella, Y.; Stephan, O.; Baldeck, P. L.; Andraud, C.; Two-photon absorption and optical limiting of bifluorene molecule. *J. Chem. Phys.*, **2001**, *114*, 5391-5396; (b) Bellier, Q.; Makarov, N. S.; Bouit, P. A.; Rigaut, S.; Kamada, K.; Feneyrou, P.; Berginc, G.; Maury, O.; Perry; J. W.; Andraud, C. Excited state absorption: a key phenomena for the improvement of biphotonic based optical limiting at telecomunication wavelengths. *Phys. Chem. Chem. Phys.*; **2012**, *14*, 15299-15307.

[20] Cumpston, B. H.; Ananthavel, S. P.; Barlow, S.; Dyer, D. L.; Ehrlich, J. E.; Erskine, L. L.; Heikal, A. A.; Kuebler, S. M.; Lee, I. Y. S.; McCord-Maughon, D.; Qin, J. Q.; Rockel, H.; Rumi, M.; Wu, X. L.; Marder, S. R.; Perry, J. W. Two-photon polymerization initiators for three-dimensional optical storage and microfabrication *Nature*, **1999**, *398*, 51-54.

[21] (a) Collins, H. A.; Khurana, M.; Moriyama, E. H.; Mariampillai, A.; Dahlstedt, E.; Balaz, M.; Kuimova, M. K.; Drobizhev, M.; Yang, V. X. D.; Phillips D.; Rebane, A.; Wilson, B. C.; Anderson, H. L.; Blood-vessel closure using photosensitizers engineered for two-photon excitation. *Nat. Photonics*, **2008**, *2*, 420-424; (b) Frederiksen, P. K.; Jorgensen, M.; Ogilby, P. R. *J. Am. Chem. Soc.* **2001**, *123*, 1215-1221; (c) Hammerer, F.; Garcia, G.; Chen, S.; Poyer, F.; Achelle, S.; Fiorini-Debuischert, C.; Teulade-Fichou, M.-P.; Maillard, P. Synthesis and characterization of glycoconjugated porphyrin triphenylamine hybrids for targeted two-photon photodynamic therapy. *J. Org. Chem.* **2014**, *79*, 1406-1417.

Accepted manuscript

[22] (a) Leo, F.; Coen, S.; Kockaert, P.; Gorza, S.-P.; Emplit, P.; Haelterman, M. Temporal cavity solitons in one-dimentional Kerr media as bits in an all-optical buffer. *Nat. Photonics* **2010**, *4*, 471-476; (b) Yabu, T.; Geshiro, M.; Kitamura, T.; Nishida, K.; Sawa, S. All-optical logic gates containing a two-mode nonlinear waveguide. *IEEE J. Quantum Electron.*, **2002**, *38*, 37-46; (c) Dinu, M.; Quochi, F.; Garcia, H. Third-order nonlinearities in silicon at telecom wavelengths *Appl. Phys. Lett.*, **2003**, *82*, 2954-2956.

[23] Xu, C.; Webb, W. W. Measurement of two-photon excitation cross-sections of molecular fluorophores with data from 690 to 1050 nm. *J. Opt. Soc. Am. B*, **1996**, *13*, 491-491.

[24] Ajami, A.; Husinsky, W.; Liska, R.; Pucher, N. Two-photon absorption cross-section measurements of various two-photon initiators for ultrashort laser radiation applying the Z-scan technique. *J. Opt. Soc. Am. B* **2010**, *27*, 2290-2297.

[25] Yin, M.; Li, H. P.; Tang, S. H. ; Ji ; W. Determination of nonlinear absoption and refraction by single Z-scan method. *Appl. Phys. B Lasers Opt.*, **2000**, *70*, 587-591.

[26] Katan, C.; Terenziani, F.; Mongin, O.; Werts, M. H. V.; Porrès L.; Pons, T.; Mertz, J.; Tretiak, S.; Blanchard-Desce, M. Effects of (multi)branching of dipolar chromophores on photophysical properties and two-photon absorption *J. Phys. Chem. A*, **2005**, *109*, 3024-3037.

[27] (a) Terenziani, F.; Katan, C.; Badaeva, E.; Tretiak, S.; Blanchard-Desce, M. Enhanced two-photon absorption of organic chromophores: theoretical and experimental assessments. *Adv. Mater.* **2008**, *20*, 4641-4678; (b) Terenziani, F.; Le Droumaguet, C.; Katan, C.; Mongin, O.; Blanchard-Desce M. Effect of branching on two-photon bsorption in triphenylbenzene derivatives. *ChemPhysChem* **2007**, *8*, 723-734; (c) Klikar, M.; Seintis, K.; Polyzos, I.; Pytela, O.; Mikysek, T.; Almonasy, N. ; Fakis, M. ; Bureš, F. Star-shaped push-pull molecules with a varied number of peripheral acceptors: an insight into their optoelectronic features. *ChemPhotoChem*, **2018**, *2*, 465-474.

Accepted manuscript

[28] (a) Lagoja, I. M.; Pyrimidine as constituent of natural biologically active compounds *Chem. Biodiv.*, **2005**, *2*, 1-50: (b) Elkanzi, N. A. A.; Zahou, F. M. Mini review on synthesis of different pyrimidine derivatives and their biological activity. *Heterocycl. Lett.* **2020**, *10*, 131-151.

[29] Hansch, C.; Leo, A.; Taft, R. W.; A survey of Hammett sustituent constants and resonance and field parameters *Chem. Rev.,* **1991**, *91*, 165-195.

[30] (a) Achelle, S.; Rodríguez-López, J.; Robin-le Guen, F. Photoluminescence properties of aryl- arylvinyl- and arylethynylpyrimidine derivatives. *ChemistrySelect*, **2018**, *3*, 1852-1886 ; (b) Lipunova, G. N.; Nosova, E. V.; Charushin, V. N.; Chupakhin, O. N. Functionalized quinazolines and pyrimidines for optolectroinc materials *Curr. Org. Synth.*, **2018**, *15*, 793-814; (c) Komatsu R.; Sasabe, H.; Kido, J. Recent progress of pyrimidine derivatives for high-performance organic light-emitting devices *J. Photonics Energy* **2018**, *8*, 032108; (d) Achelle, S.; Baudequin, C. Recent advances in pyrimidine derivatives as luminescent, photovoltaic and nonlinear optical materials *Target Heterocycl. Syst.*; **2013**, *17*, 1-34.

[31] (a) Itami, K.; Yamazaki, D.; Yoshida, J.; Pyrimidine-core extended pi-systems: general synthesis and interesting fluorescent properties *J. Am. Chem. Soc.,* **2004**, *126*, 15396-15397; (b) Achelle, S.; Nouira, I.; Pfaffinger, B.; Ramondenc, Y.; Plé, N.; Rodríguez-López, J. V-shaped 4,6-bis(arylvinyl)pyrimidine oligomers : synthesis and optical properties. *J. Org. Chem.* **2009**, *74*, 3711-3717; (c) Kato, S.-I.; Yamada, Y.; Hiyoshi, H.; Umezu, K.; Nakamura, Y. Series of carbazole-pyrimidine conjugates: syntheses and electronic, photophysical, and electrochemical properties. *J. Org. Chem.*, **2015**, *80*, 9076-9090; (d) Rodríguez-Aguilar, J.; Vidal, M.; Pastenes, C.; Aliaga, C.; Rezende, M. C.; Dominguez, M. The solvatofluorochromsims of 2,4,6-triarylpyrimidine derivatives *Photochem. Photobiol.*, **2018**, *94*, 1100-1108 ; (e) Fecková, M.; le Poul, P.; Robin-le Guen, F.; Roisnel, T.; Pytela, O.;

Accepted manuscript

Klikar, M.; Bureš, F. Achelle, S. 2,4-distyryl- and 2,4,6-tristyrylpyrimidines : synthesis and photophysical properties. *J. Org. Chem.* **2018**, *83*, 11712-11726.

[32] Achelle, S.; Rodríguez-López, J.; Bureš, F.; Robin-le Guen, F. Tuning the photophysical properties of push-pull Azaheterocyclic chromophores by protonation : a brief overview of a French-Spanish-Czech project *Chem. Rec.* **2020** *in press* doi: 10.1002/tcr.201900064

[33] Hadad, C.; Achelle, S.; López-Solera, I.; García-Martínez, J. C. Rodríguez-López, J. Metal cation complexation studies of 4-arylvinyl-2,6-di(pyridin-yl)pyrimidines : effect on the optical properties. *Dyes Pigm.,* **2013**, *97*, 230-237.

[34] Aranda; A. I.; Achelle, S.; Hammerer, F. ; Mahuteau-Betzer, F.; Teulade-Fichou, M.-P. Vinyl-diazine triphenylamine and their N-methylated derivatives : Synthesis photophysical properties and application for stainig DNA. *Dyes Pigm.*, **2012**, *95*, 400-407.

[35] (a) Schomaker, J. M.; Delia, T. J. Arylation of halogenated pyrimidines via a Suzuki coupling reaction *J. Org. Chem.*, **2001**, *66*, 7125-7128; (b) Achelle, S.; Ramondenc, Y.; Dupas, G.; Plé, N. Bis and tris(arylethynyl)pyrimidine oligomers : synthesis and light-emitting properties. *Tetrahedron* **2008**, *64*, 2783-2791.

[36] Pascal, L.; Vanden Eynde, J. J.; Van Haverbeke, Y.; Dubois, P.; Michel, A.; Rant, U. ; Zojer, E. ; Leising, G. ; Van Dorn, L. O.; Gruhn, N. E.; Cornil, J.; Brédas, J. L. Synthesis and characterization of novel para- and meta-phenylenevinylene derivatives: fine tuning of the electronic and optical properties of conjugated materials. *J. Phys. Chem. B* **2002**, *106*, 6442-6450.

[37] (a) Kanna, R.; He, G. S.; Lin, T. C.; Prasad, P. N.; Vaia, R. A.; Tan, L. S. Toward highly active two-photon absorbing liquids. Synthesis and characterization of 1,3,5-triazine-based octopolar molecules. *Chem. Mater.*, **2004**, *16*, 15-194; (b) Jiang, Y. H.; Wang, Y. C.; Wang, B.; Yang, J.; He, N.; Qian, S.; Hua, J.; Synthesis, two-photon absorption and optical limiting properties of multi-branched styryl derivatives based on 1,3,5-triazine *Chem. Asian J.*, **2011**,

Accepted manuscript

6, 157-165; (c) Ren, S.; Zeng, D;; Zhong, H.; Wang, Y.; Qian, S.; Fang, Q. Star-shaped donor-pi-acceptor conjugated oligomers with 1,3,5-triazine cores: convergent synthesis and multifunctional properties. *J. Phys. Chem. B*, **2010**, *114*, 10374-10383.

[38] (a) Achelle, S.; Barsella, A.; Baudequin, C.; Caro, B.; Robin-le Guen, F. Synthesis and Photophysical Investigation of a Series of Push−Pull Arylvinyldiazine Chromophores. *J. Org. Chem.* **2012**, *77*, 4087-4096. (b) Achelle, S.; Kahlal, S.; Barsella, A.; Saillard, J. Y.; Che, X.; Vallet, J.; Bureš, F.; Caro, B.; Robin-Le Guen, F. Improvement of the quadratic non-linear optical properties of pyrimidine chromophores by *N*-methylation and tungsten pentacarbonyl complexation. *Dyes Pigm.* **2015**, *113*, 562-570. ; (c) Castet, F.; Pic, A.; Champagne, B. Linear and nonlinear optical properties of arylvinyldiazine dyes: A theoretical investigation *Dyes Pigm.* **2014**, *110*, 256-260.

[39] Achelle, S.; Barsella, A.; Caro, B.; Robin-Le Guen, F. Donor–linker–acceptor (D–p–A) diazine chromophores with extended p-conjugated cores: synthesis, photophysical and second order nonlinear optical properties *RSC Adv.* **2015**, *5*, 39218-39227.

[40] (a) Jen, A. K.-Y.; Rao, P.; Wong, K. Y.; Drost, K. J. Functionalized thiophenes : second-order nonlinear optics materials. *J. Chem. Soc., Chem. Commun.* **1993**, 90-92. ; (b) Rao, V. P.; Cai, Y. M.; Jen. A. K.-Y. Ketene dithioacetal as a π-electron donor in second-order nonlinear optical chromophores. *J. Chem. Soc., Chem. Commun.* **1994**, 1689-1690. ; (c) Wong, K. Y.; Jen, A. K.-Y.; Rao, V. P.; Drost, K. J. Theoretical and experimental studies of the molecular second order nonlinear optical response of heteroaromatic compounds. *J. Chem. Phys.* **1994**, *100*, 6818-6825. ; (d) Kulhánek, J.; Bureš, F.; Opršal, J.; Kuznik. W.; Mikýsek, T.; Růžička, A. 1,4-Phenylene and 2,5-thienylene π-linkers in charge-transfer chromophores. *Asian J. Org. Chem.* **2013**, *2*, 422-431.

[41] (a) Senge, M. O.; Fazekas, M.; Notara, E. G. A.; Blau, W. J.; Zawadzka, M.; Locos, O. B.; Mhuircheartaigh E. M. N. Nonlinear optical properties of porphyrins. *Adv. Mater.* **2007**, *19*,

Accepted manuscript

2737-2774. ; (b) Delgado, M. C. R.; Casado, J.; Hernandes, V.; Navarrete, J. T. L.; Orduna, J.; Villacampa, B.; Alicante, R.; Raimundo, J. M.; Blanchard, P.; Roncali, J. Electronic, optical, and vibrational properties of bridged dithienylethylene-based NLO chromophores. *J. Phys. Chem. C* **2008**, *112*, 3109-3120. ; (c) Liu, J.; Gao, W.; Kityk I. V.; Liu, X.; Zhen, Z. Optimization of polycyclic electron-donors based on julolidinyl structure in push-pull chromophores for second order NLO effects. *Dyes Pigm*. **2015**, *122*, 74-84; (d) Seferoglu, Z. Recent Synthetic Methods for the Preparation of Charged and Uncharged Styryl-based NLO Chromophores: A Review. *Org. Prep. Proced. Int.* **2017**, *49*, 393-337. ; (e) Rajeshirke, M.; Sekar, N. Multi-stimuli responsive emissive NLOphoric colorants – A recent trend in research. *Dyes Pigm.* **2019**, *163*, 675-683.

[42] Marder, S. R.; Beratan, D. N.; Cheng, L.-T. Approaches for Optimizing the First Electronic Hyperpolarizability of Conjugated Organic Molecules *Science* **1991**, *252*, 103-106.

[43] (a) Achelle, S.; Malval, J.-P.; Aloiṡe, S.; Barsella. A.; Spangenberg, A.; Mager, L.; Akdas-Kilig, H.; Fillaut, J.-L.; Caro, B.; Robin-Le Guen, F. Synthesis, Photophysics and Nonlinear Optical Properties of Stilbenoid Pyrimidine-Based Dyes Bearing Methylenepyran Donor Groups. *ChemPhysChem.* **2013**, *14*, 2725-2736. ; (b) Durand, R. J.; Achelle, S.; Gauthier, S.; Cabon, N.; Ducamp, M.; Kahlal, S.; Saillard, J.-Y.; Barsella, A.; Robinn-Le Guen, F. Incorporation of a ferrocene unit in the π-conjugated structure of donor-linker-acceptor (D-π-A) chromophores for nonlinear optics (NLO). *Dyes Pigm.* **2018**, *155*, 68-74. ; (c) Durand, R. J.; Gauthier, S.; Achelle, S.; Kahlal, S.; Saillard, J.-Y.; Barsella, A.; Wojcik, L.; Le Poul, N.; Robin-Le Guen, F. Incorporation of a platinum center in the pi-conjugated core of push–pull chromophores for nonlinear optics (NLO). *Dalton Trans.* **2017**, *46*, 3059-3069. ; (d) Durand, R. J.; Gauthier, S.; Achelle, S.; Groizard, T. ; Kahlal, S.; Saillard, J.-Y.; Barsella, A.; Le Poul, N.; Robin-Le Guen, F. Push–pull D–π-Ru–π-A chromophores: synthesis and electrochemical,

Accepted manuscript

photophysical and secondorder nonlinear optical properties. *Dalton Trans.* **2018**, *47*, 3965–3975.

[44] Cifuentes, M. P.; Humphrey, M. G. Alkynyl compounds and nonlinear optics. *J. Organomet. Chem.* **2004**, *689*, 3968-3981.

[45] Klikar, M.; Le Poul, P.; Růžička, A.; Pytel, O.; Barsella, A.; Dorkenoo, D. K.; Robin-Le Guen, F.; Bureš, F.; Achelle, S. Dipolar NLO Chromophores Bearing Diazine Rings as π-Conjugated Linkers. *J. Org. Chem.* **2017**, *82*, 9645-9451.

[46] He, M.; Zhou, Y.; Liu, R.; Dai, J.; Cui, Y.; Zhang, T. Novel nonlinearity–transparency–thermal stability trade-off of thiazolylazopyrimidine chromophores for nonlinear optical application. *Dyes Pigm.* **2009**, *80*, 6-10.

[47] (a) Van Cleuvenbergen, S.; Kędziora, P.; Fillaut, J.-L.; Verbiest, T.; Clays, K.; Akdas-Kiliç, H.; Camerel, F. Chiral Side Groups Trigger Second Harmonic Generation Activity in 3D Octupolar Bipyrimidine-Based Organic Liquid Crystals. *Angew. Chem. Ind. Ed.* **2017**, *56*, 9546-9550. ; (b) Akdas-Kiliç, H.; Gafroy, M.; Fillaut, J.-L.; Donnio, B.; Heinrich, B.; Kędziora, P.; Malval, J.-P.; Spangenberg, A.; Van Cleuvenbergen, S.; Clays, K.; Camerel, F. Mesogenic, Luminescence, and Nonlinear Optical Properties of New Bipyrimidine-Based Multifunctional Octupoles. *J. Phys. Chem. C* **2015**, *119*, 3697-3710. ; (c) Akdas-Kiliç, H.; Roisnel, T.; Ledoux, I.; Le Bozec, H. A new class of bipyrimidine-based octupolar chromophores: synthesis, fluorescent and quadratic nonlinear optical properties. *New J. Chem.* **2009**, *33*, 1470-1473.

[48] Doddamani, R. V.; Rachipudi, P. S. ; Inamdar, S. R. ; Kariduraganavar, M. Y. Enhancement of nonlinear optical and thermal properties of polyurethanes by modifying the chromophores with fused heterocyclic and pyrimidine rings *Polym. Eng. Sci.* **2019**, *59*, 500-509

Accepted manuscript

[49] (a) Li, L. ; Tian, Y. ; Yang, J.-X. ; Sun P.-P.; Wu, J.-Y.; Zhou, H.-P.; Zhang, S.-Y.; Jin, B.-K.; Xing, X.-J.; Wang, C.-K.; Li, M.; Cheng, G.-H.; Tang, H.-H.; Huang, W.-H.; Tao, X.-T.; Jiang, M.-H. Facile synthesis and systematic investigation of a series of novel bent-shapped two-photon absortion chromophores based on pyrimidine *Chem. Asian J.* **2009**, *4*, 668-680. (b) Liu, D.-F.; Wang, F.-W.; Wu, K. N.; Li, W.; Sun, Y.-P. ; Wang, C ;-K. Facile synthesis, optical properties and theoretical calculation of a novel bent-shaped two-photon absortion chromophore *Phys. Chem. Liquids* **2010**, *48*, 99-107.

[50] Liu, B.; Hu, X.-L.; Liu, J.; Zhao, Y.-D.; Huang, Z. L. Synthesis and photophysical properties of novel pyrimidine-based two-photon absorption chromophores. *Tetrahedron Lett.* **2007**, *48*, 5958-5962.

[51] Zhang, Q. ; Luo, L. ; Xu, H. ; Hu, Z. ; Brommesson, C. ; Wu, J. ; Sun, Z. ; Tian, Y. ; Uvdal, K. Design, synthesis, linear and nonlinear photophysical properties of novel pyrimidine-based imidazole derivatives *New J. Chem.* **2016**, *40*, 3456-3463.

[52] Zhang, Q.; Tian, X.; Wang, H.; Hu, Z.; Wu, J.; Zhou, H.; Zhang, S.; Yang, J.; Sun, Z.; Tian, Y. NIR-region two-photon fluorescent probes for Fe^{3+}/Cu^{2+} ions based on pyrimidine derivatives with different flexible chain. *Sensors Actuators B: Chem.* **2016**, *222*, 574-578.

[53] Tang, C.; Zhang, Q.; Li, D.; Zhang, J.; Shi, P.; Li, S.; Wu, J.; Tian, Y. Synthesis, crystal structures, two-photon absorption and biological imaging application of two-novel bent-shaped pyrimidine derivatives. *Dyes Pigm.* **2013**, *99*, 20-28

[54] Zhang, Q.; Tian, X.; Hu, Z.; Brommesson, C.; Wu, J.; Zhou, H.; Yang, J.; Sun, Z.; Tian, Y.; Uvdal, K. Nonlinear optical response and two-photon biological applications of a new family of imidazole-pyrimidine derivatives. *Dyes Pigm.* **2016**, *126*, 286-295.

[55] (a) Achelle, S.; Saettel, N.; Baldeck, P.; Teulade-Fichou M.-P.; Maillard, P. Bisporphyrin connected by pyrimidine: synthesis and photophyscal properties. J. *Porphyrins*

Accepted manuscript

Phthalocyanines **2010**, *14*, 877-884; (b) Jiblaoui, A.; Brevier, J.; Ducourthial, G.; González-Núñez, H.; Baudequin, C.; Sol, V.; Leroy-Lhez, S. Modulation of intermolecular interactions in new pyrimidine-porphyrin system as two-photon absorbing photosensitizers. *Tetrahedron*, **2015**, *71*, 2428-2434.

[56] Drobizhev, M.; Stepanenko, Y.; Dzenis, Y.; Karotki, A.; Rebane, A.; Taylor, P. N.; Anderson, H. L. Extremely stron near IR Two-photon absorption in conjugated porphyrin dimmers: quantitative description with three-essential state model. *J. Phys. Chem. B* **2005**, *109*, 7223-7236.

[57] Hammerer, F.; Achelle, S.; Baldeck, P.; Maillard, P.; Teulade-Fichou, M.-P. Influence of carbohydrate biological vector on the two-photon resonance of porphyrin oligomers J. *Phys. Chem. A* **2011**, *115*, 6503-6508.

[58] Bureš, F. Fundamental aspects of perperty tuning in push-pull molecules *RSC Adv.* **2014**, *4*, 58826-58851.

[59] Chen, D.; Zhong, C.; Dong, X.; Liu, Z.; Qi, J. A new building block, bis(thiophene vinyl)-pyrimidine, for constructing excellent two-photon absorption materials: synthesis, crystal structure and properties. *J. Mater. Chem.* **2012**, *22*, 4343-4348.

[60] Cvejn, D.; Achelle, S.; Pytela, O.; Malval, J.-P. ; Spangenberg, A. ; Cabon N. ; Bureš, F. ; Robin-le Guen, F. Tripolal molecules with triphenylamine core, diazine peripheral groups and extended π-conjugated linkers. *Dyes Pigm.* **2016**, *124*, 101-109.

[61] Savel, P.; Akdas-Kiliç, H.; Malval, J.-P.; Spangenberg, A.; Roisnel, T.; Fillaut, J.-L. Metal-induced dimentionality tuning in a series of bipyrimidine-based ligands: a tool to enhance two-photon absorption *J. Mater. Chem. C* **2014**, *2*, 295-305.

[62] Denneval, C.; Moldovan, O.; Baudequin, C.; Achelle, S.; Baldeck, P.; Plé, N.; Darabantu, M.; Ramondenc, Y. Synthesis and photophysical properties of push-pull structures

Accepted manuscript

incorporating diazines as attracting part with a fluorine core. *Eur. J. Org. Chem.* **2013**, 5591-5602

[63] Liu, Z.; Chen, T.; Liu, B.; Huang, Z.-L. ; Huang, T. ; Li, S. ; Xu, Y. ; Qin, J. Two-photon absorption of a series of V-shape molecules : the influence of acceptor's strength on two-photon absorption in a noncentrosymmetric D-π-A-π-D system. *J. Mater. Chem.* **2017**, *17*, 4685-4689.

[64] Zhang, Q.; Luo, J.; Ye, L.; Wang, H.; Huang, B.; Zhang, J.; Wu, J.; Zhang, S.; Tian, Y. Design, synthesis, linear and nonlinear photophysical properties and biological imaging application of a novel Λ-type pyrimiine-based thiophene derivative *J. Mol. Struct.* **2014**, *1074*, 33-42.

[65] Yang, J.; Hu, W.; Li, H.; Hou, H. ; Tu, Y. ; Liu, B. Facile synthesis of a two-photon fluorescent probe based on pyrimidine 2-isocyanate and its application in bioimaging. *Photochem. Photobiol. Sci.* **2018**, *17*, 474-481.

[66] Kournoutas, F. ; Fihey, A. ; Malval, J.-P. ; Spangenberg, A. ; Fecková, M.; le Poul, P.; Katan, C. ; Robin-le Guen, F. ; Bureš, F. ; Achelle, S. ; Fakis, M. Branching effect on the linear and non linear optical properties of styrylpyrimidines *Phys. Chem. Chem. Phys.* **2020**, *22*, 4167-4176.

[67] Wang, H.; Zhang, Q.; Zhang, J.; Li, L.; Zhang, Q.; Li, S.; Zhang, S.; Wu, J.; Tian, Y. Synthesis, two-photon absorption properties and bioimaging application of mono-, di- and hexa-branched pyrimidine derivatives Dyes *Pigm.* **2014**, *102*, 263-272.

[68] Latouche, C.; Akdas-Kilig, H.; Malval, J.-P.; Fillaut, J.-L.; Boucekkine, A.; Barone, V. Theoretical evidence of metal-induced structural distortions in a series of bipyrimidine-based ligands. *Dalton Trans.* **2015**, *44*, 506-510.

Accepted manuscript

[69] Chen, D. ; Zhong, C. ; Zhao, Y. ; Nan, L.; Liu, Y.; Qin, J. A two-dimentional molecule with large conjugation degree: synthesis, two-photon absorption and charge transport ability *J. Mater. Chem. C*, **2017**, *5*, 5199-5206.

[70] Verlhac J.-B.; Daniel, J.; Pagano, P.; Clermont, G. ; blanchard-Desce, M. Enanced two-photon brighness in molecular-based organic nanoparticles built from articulated-dipoles *C. R. Chim.*, **2016**, *19*, 28-38.

[71] Liu, Z. ; Xiong, X. ; Li, Y. ; Li, S.; Qin, J. Synthesis, optical properties and singlet oxygen generation of a phthalocyanine derivative containing strong two-photon absorbing chromophores in the periphery *Photochem. Photobiol Sci.*, **2011**, *10*, 1804-1809.

[72] Li, L. ; Tian, Y. ; Yag, J. ; Sun, P.; Kong, L.; Wu, J.; Zhou, H.; Zhang, S.; Jin, B.; Tao, X.; Jiang, M. Two-photon absorption enhancement induced by aggregation with accurate photophysical data: spontaneous accumulation of dye in silica nanoparticules. *Chem. Commun.* **2010**, *46*, 1673-1675.

[73] Malval, J.-P.; Achelle, S.; Bodiou, L.; Spangenberg, A.; Gomez, L. C.; Soppera, O.; Robin-le Guen, F. Two-photon absorption in a conformationally twisted D-π-A oligomer: a synergic photosensitizing approach for multiphoton lithography *J. Mater. Chem. C*, **2014**, *2*, 7869-7880.

[74] Liu, B. ; Zhang, H.-L. ; Liu, J. ; Zhao, Y.-D.; Luo, Q.-M.; Huang, Z.-L. Novel pyrimidine-based amphiphilic molecules: synthesis, spectroscopic properties and application in two-photon fluorescence microscopic imaging *J. Mater. Chem.* **2007**, *17*, 2921-2929.

[75] Zhang, Q.; Guan, R.; Tian, X.; Luo, L.; Zhou, H.; Li, S.; Wu, J.; Tian, Y. Small water-soluble pyrimidine hexafluorophosphate derivatives with high two—photon absorption activities in the near-IR region and their biological applications. *RSC Adv.* **2017**, *7*, 20068-20075.

Accepted manuscript

[76] Hu, L.; Hussain, S.; Liu, T.; Yue, Y. ; Liu, J.; Tian, Y.; Tian, X. A molecular probe based on pyrimidine imidazole derivatives for stable super-resolution endoplasmic reticulum imaging in living cells. *New J. Chem.* **2018**, *42*, 14725-14728.

[77] Zhang, Q.; Li, L.; Zhang, M.; Liu, Z.; Wu, J.; Zhou, H.; Yang, J.; Zhang, S.; Tian, Y. Nonlienar optical response and biological applications of a series of pyrimidine-based molecules for copper(II) ion probe *Dalton Trans.* **2013**, *42*, 8848-8853.

[78] Li L.; Ge, J.; Wu, H.; Xu, Q.-H.; Yao, S. Q. Organelle-specific detection of phosphatase activities with two-pphoton fluorogenic probes in cells and tissues. *J. Am. Chem. Soc.* **2012**, *134*, 12157-12167.

[79] Doan, P. H. ; Pitter, D. R. G.; Kocher, A.; Wilson, J. N.; Goodson II T. Two-photn spectroscopy as new sensitive method for determining the DNA binding mode of fluorescent nuclear dyes. *J. Am. Chem. Soc.* **2015**, *127*, 9198-9201.

[80] Cai, J.; Huang, W. Two-photon three-dimensional optical storage of a new pyrimidine photobleaching material *Optik*, **2015**, *126*, 343-346.

[81] (a) Wang, A.; Long, L.; Meng, S.; Li, X.; Zhao, W.; Sog, Y.; Cifuentes, M. P.; Humphrey, M. G.; Zhang, C. Cooperative enhancement of optical nonlinearities in a porphyrin derivative bearing a pyrimidine chromophore at the preriphery *Org. Biomol. Chem.* **2013**, *11*, 4250-4257; (b) Zou, Y.; Zhang, Q.; Showkot Hossain, A. M.; Li, S.-L.; Wu, J.-W.; Ke, W.-Z.; Jin, B.-K.; Yang, J.-X.; Zhang, S.-Y.; Tian, Y. Synthesis, crystal structure, electrochemistry and nonlinear optical properties of a novel (D-A-D) biferrocenyl derivative: 2-amino-4,6-diferrocenylpyrimidine *J. Organometallic Chem.* **2012**, *720*, 66-72.

[82] Ge, J.-F.; Lu, Y.-T.; Sun, R.; Zhang, J. ; Xu, Q.-F. ; Li, N.-J. ; Song, Y.-L. ; Lu, J.-M. Third-order nonlinear optical properties of symmetric phenoxazinium chlorides with resonance structures at 532 nm *Dyes Pigm.* **2011**, *91*, 489-494.

Accepted manuscript

[83] Karuppasamy, P. ; Kamalesh, T. ; Anitha, K. ; Abdul Kalam, S.; Pandian, M. S.; Ramasamy, P.; Verma, S.; Rao, S. V. Synthesis, crystal growth, structure and characterization of a novel third order nonlinear optical organic single crystal: 2-amino 4,6-dimethylpyrimidine 4-nitrophenol. *Opt. Mater.* **2018**, *84*, 475-489.

Accepted manuscript